ADVANCED MATERIALS TECHNOLOGIES
www.advmattechnol.de

Trending Technology of Glucose Monitoring during COVID-19 Pandemic: Challenges in Personalized Healthcare

Le Minh Tu Phan, Thuy Anh Thu Vo, Thi Xoan Hoang, Sathish Panneer Selvam, Hoang Lan Pham, Jae Young Kim, and Sungbo Cho**

The COVID-19 pandemic has continued to spread rapidly, and patients with diabetes are at risk of experiencing rapid progression and poor prognosis for appropriate treatment. Continuous glucose monitoring (CGM), which includes accurately tracking fluctuations in glucose levels without raising the risk of coronavirus exposure, becomes an important strategy for the self-management of diabetes during this pandemic, efficiently contributing to the diabetes care and the fight against COVID-19. Despite being less accurate than direct blood glucose monitoring, wearable noninvasive systems can encourage patient adherence by guaranteeing reliable results through high correlation between blood glucose levels and glucose concentrations in various other biofluids. This review highlights the trending technologies of glucose sensors during the ongoing COVID-19 pandemic (2019–2020) that have been developed to make a significant contribution to effective management of diabetes and prevention of coronavirus spread, from off-body systems to wearable on-body CGM devices, including nanostructure and sensor performance in various biofluids. The advantages and disadvantages of various human biofluids for use in glucose sensors are also discussed. Furthermore, the challenges faced by wearable CGM sensors with respect to personalized healthcare during and after the pandemic are deliberated to emphasize the potential future directions of CGM devices for diabetes management.

1. Introduction

Between 2019 and 2020, coronavirus disease (COVID-19) pandemic has rapidly spread worldwide, leading to millions of infection cases and a mortality rate of 5.7%.[1] Diabetes is considered a risk factor for many serious infections, especially for the rapid progression and poor prognosis of COVID-19, and thus, patients with diabetes require more intensive attention.[2,3] This has created a considerable clinical challenge for diabetes management during the ongoing pandemic. To prevent the risk of coronavirus transmissions, remote monitoring of glucose levels is required to provide personalized homecare. Thus, the development of personalized continuous glucose monitoring (CGM) has attracted more attention during this pandemic to efficiently manage diabetes and avoid the spread of coronavirus.[4] Therefore, in the context of these unprecedented times, telemedicine intervention in support of CGM would be an ideal solution for diabetes management, enabling remote clinical consultation for patients with diabetes via glucose self-monitoring with the support of personalized CGM devices, not only remaining the efficacy in diabetes care but limiting exposures to coronavirus between patients and residents to contribute to global efforts against coronavirus.

Glycemic control, a vital consideration for diabetes care, is recommended to be personalized[5] to control diabetes, becoming more important during COVID-19 pandemic. Diabetic complications typically arise owing to acute hyperglycemic fluctuations,[6] which are frequently neglected due to single-use blood glucose measurement. Although blood glucose monitoring is accurate for the diabetes management because of high precision, miniaturization, and robust production of devices, it is still challenging to track fluctuations in glucose levels during daily activities without increasing the risk of coronavirus infection through timely communication with patients with diabetes mellitus. To address this problem, CGM devices have been developed and commercialized to provide an effective alternative glucose measurement method that can monitor real-time changes in blood glucose concentration. However,

Prof. L. M. T. Phan, S. P. Selvam, Prof. S. Cho
Department of Electronic Engineering
Gachon University
Seongnam-si, Gyeonggi-do 13120, Republic of Korea
E-mail: plmtu@smp.udn.vn; sbcho@gachon.ac.kr
Prof. L. M. T. Phan
School of Medicine and Pharmacy
The University of Danang
Danang 550000, Vietnam
T. A. T. Vo, Prof. T. X. Hoang, H. L. Pham, Prof. J. Y. Kim
Department of Life Science
Gachon University
Seongnam-si, Gyeonggi-do 461-701, Republic of Korea
Prof. S. Cho
Department of Health Sciences and Technology
GAIHST
Gachon University
Incheon 21999, Republic of Korea
The ORCID identification number(s) for the author(s) of this article can be found under https://doi.org/10.1002/admt.202100020.

DOI: 10.1002/admt.202100020

 © 2021 Wiley-VCH GmbH

CGM devices have some limitations in terms of cost, accuracy, and patient friendliness,[7] which has led to the development of wearable noninvasive glucose-monitoring platforms. In recent years, wearable glucose-monitoring platforms using different human biofluids have been developed, and these have shown suitable compatibility with blood glucose levels. The development and application of these wearable CGM devices are in the pioneering phase, and certain shortcomings remain regarding the clinical utilization for point-of-care monitoring. Under the pressure of COVID-19 pandemic, wearable CGM-based personalization of diabetes healthcare has faced difficulties in offering considerable management significance to the hospital healthcare system, leading the researchers to make an effort to develop superior glucose sensors that are applicable from hospital to home for contribution in the fight against coronavirus.

In this review, we highlight the trending technologies of glucose measurement for personalized healthcare monitoring systems for patients with diabetes during COVID-19 pandemic. The latest progress from 2019 to 2020 of glucose monitoring platforms that have been developed to significantly contribute to a global effort on tackling COVID-19 as well as managing diabetes was reviewed, representing the possibilities of nanomaterials toward glucose monitoring, from invasive to noninvasive measurement, by comparing the sensing performance in terms of materials, sensitivity, and time response. In addition, the benefits and drawbacks of various human biofluids in glucose sensing are discussed to deliberate the challenges of wearable CGM devices, from the perspective of universalization to personalization toward personalized healthcare systems owing to the support of wearable CGM technology during this pandemic and in the future.

2. Off-Body Sensors for Glucose Monitoring

Most of conventional blood glucose measurements involving common handheld glucometers required a finger pricked step to prepare blood samples through a disposable test strip based on enzymatic reaction.[8] Despite the quite accurate performance, especially during the COVID-19 pandemic, the overwhelming need for continuous glucose monitoring, which is accurate enough to help health-care workers control diabetes, attacks considerable attention of scientists. To address the disadvantages of glucometers and improve the comfort and compliance of patients, scientists are attempting to fabricate more effective sensing platforms using either enzymatic or nonenzymatic methods. To satisfy the demand of affordable and convenient glucose-monitoring sensors for diabetes management; thus, an attempt was made to investigate glucose-sensing optimization. Electrochemical and optical sensing platforms for glucose measurement are the most popular investigated due to their advantages in term of sensitivity, selectivity, and stability that can be utilized to be an efficient CGM device.[9,10]

2.1. Nanomaterial-Based Optical Glucose Sensors

Signals for optical biosensing are either directly generated via the interaction of the biorecognition element and the optical field, or via label-free techniques. Transduction systems of optical sensing are diverse, that include fluorescence/near-infrared (NIR) fluorescence and surface-enhanced Raman scattering (SERS) spectroscopy.[9] Particularly, for recognition of biological entities, various biomolecules can be employed, such as enzymes, antigens/antibodies, hormone receptors, or nuclear acids that are recognized through catalysis or affinity binding.[11,12]

Recently, most optical glucose sensors are based on the intensity of color change and on the binding of an enzyme or nanomaterial with glucose. Primitive enzymes derived from nature have been commonly used for the colorimetric determination of glucose by hydrogen peroxide (H_2O_2), which can accelerate the speed of chemical reactions due to the regulation of biological processes under mild environmental conditions.[13] Currently, various lateral flow assays (LFAs) have been employed for glucose measurement, which depends on color change when the dipstick of the sensor touches the fluid.[14] Most recent studies have employed nanocellulose (NC), an intriguing cellulose-based material, to develop a colorimetric detection system by integrating glucose oxidase (GOx) on the carboxyl-NC/cellulose substrate via TEMPO-mediated oxidation. After the carboxyl-NC is optimized, this integrated system was also underpinned by the basic principles of LFA. This detection system allowed the color change in the presence of H_2O_2 with a response range of 1.5×10^{-3} to 13.0×10^{-3} M for glucose concentrations in urine (**Figure 1**A).[15] For fluorescence systems, rational design and fluorophore are crucial factors that influence device performance.[16] Conventional strategies involve establishing glucose enzymatic oxidation by glucose oxidase by integration with various biomolecules or nanoparticles.[17–19] In recent years, biodots, also known as bioinspired fluorescent nanodots, have attracted attention in the nanochemistry field because of their inherent profiles, such as biocompatibility, favorable aqueous dispersibility, low cost, and tunable fluorescence.[18] In particular, such a platform was developed using a threonine–PEI dot (TP)–GOx glucose-monitoring system in which hydrothermal methods were used for sensing artificial sweat samples (Figure 1B).[18] In this system, the ultrasmall size of the biodot allowed it to be conjugated with GOx to minimize the protein's native function disturbance, resulting in a single-step fluorescence "turn-off" enzymatic assay. Although it has good quality in terms of sensitivity, enzymatic-based sensing has several nonignorable drawbacks such as the cost of synthesis, especially for active enzyme immobilization which depends on external environmental factors such as pH, temperature, or humidity, leading to instability and as a result a reduction in enzyme activity, and finally, influent precision of detection systems.[13,20,87] Alternatively, to overcome these drawbacks, nanozymes, which can efficiently mimic enzyme activities, are attracting attention using nonprotein molecules, including metal/metal oxide-based nanoparticles, graphene oxide, or supramolecules.[13,20,21] Diverse enzyme-like nanomaterials have been reported to contain glucose oxidase-like, superoxide dismutase-like (SOD-like), and peroxidase-like activity (the most popular) in the presence or absence of H_2O_2. Although these enzyme-mimetic nanomaterials are becoming potential candidates owing to their considerable benefits such as low cost, design flexibility, earth plentitude, and high stability under harsh conditions, they lack stability and biocompatibility in solution,

© 2021 Wiley-VCH GmbH

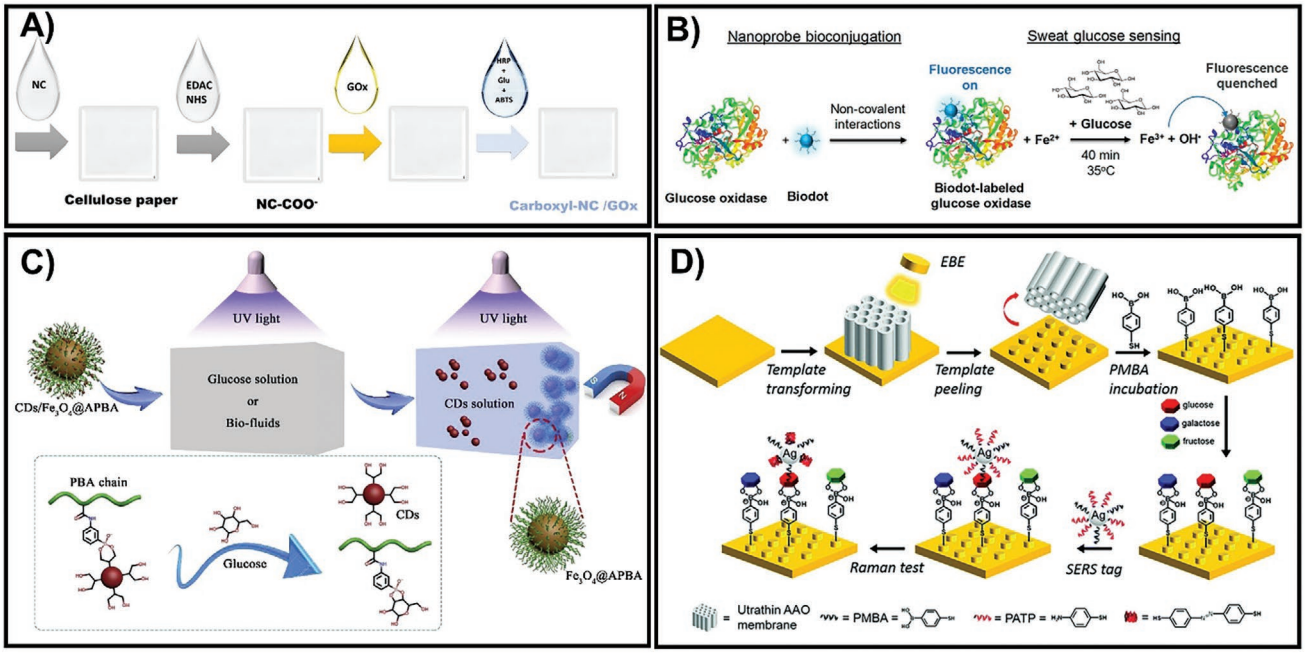

Figure 1. A) Fabrication of colorimetric-based glucose test-strip by casting the indicated solutions on cellulose substrates. Adapted with permission.[15] Copyright 2020, Elsevier. B) The formation of a one-step glucose sensor by integrating threonine–PEI dots with GOx as an enzyme-fluorescent sensing probe. Adapted with permission.[18] Copyright 2020, American Chemical Society. C) The fundamental principle of the CDs/Fe_3O_4@APBA system for blood glucose determination. Adapted with permission.[24] Copyright 2020, Elsevier. D) The preparation of the Au-ND/glucose/Ag NPs sandwich system based on the SERS principle. Adapted with permission.[25] Copyright 2021, RSC Pub.

which still pose challenges. Hence, to eliminate these shortcomings and improve the accuracy of determination, enzyme-free colorimetric detection techniques have been developed based on diverse nanomaterials including nanotubes, nanorods, nanoparticles, nanosheets, and nanowires.[13,22] Typically, Pd nanoparticles (Pd NPs) or pristine Co_3O_4 (P-Co_3O_4)/reduced Co_3O_4 (R-Co_3O_4) nanocomposites are attracting increasing attention because they possess peroxidase-like activity as well as optical properties, and thus, can be used to construct a colorimetric glucose probe. Both Pd_{91}-GBLP NPs and the P-Co_3O_4/R-Co_3O_4 platform, which are fabricated via bioconjugation or hydrothermal techniques, can monitor glucose levels at a very low limit detection of 1×10^{-6} M and 0.69×10^{-6} M/0.32×10^{-6} M, respectively.[20,23] Multi-hydroxyl carbon dots (CDs) were aggregated on phenylboronic acid (PBA)-molecular-brush-grafted magnetic nanoparticles (Fe_3O_4@APBA) to produce a novel glucose composite probe that can respond to glucose in human blood at a minimum level of 0.15×10^{-6} M within 5 min (Figure 1C).[24] In other study, Long et al. proposed a novel sandwich assay by self-assembling *p*-mercapto-phenylboronic acid (PMBA) monolayers on a gold nanodisk (Au-ND) and then mixing with silver nanoparticles (AgNPs) (Figure 1D). This system allowed the monitoring of blood glucose in the wide range of 1×10^{-3} to 40×10^{-3} M after a fast response time within 10 s.[25]

Recently, few studies have reported that optical-based glucose measurement techniques are less attractive than electrochemical-based sensors (**Table 1**). Although optical glucose-sensing systems have achieved good performance with high sensitivity and selectivity, these platforms have not attracted attention because of the long response time or lack of reusability, making it difficult to release commercially.

2.2. Nanomaterial-Based Electrochemical Sensors of Glucose

Electrochemical sensors have attracted immense attention because of their facile fabrication and miniaturization of equipment. These instruments can provide a quantifiable electric signal based on glucose levels, such as current or voltage. The devices can be classified into two types based on the sensing element—enzymatic (enzyme present) or nonenzymatic (enzyme absent).[38–40] Herein, we highlight the development of novel glucose-electrochemical sensors using diverse sensing materials containing enzymes, metal-oxide nanocomposites, bimetallic nanoparticles, carbon nanotubes, graphene-oxide-based nanomaterials, and conductive polymers, which are described in **Table 2**.

2.2.1. Novel Investigation of Enzyme-Based Electrochemical Glucose Sensors

Since the generation of glucose sensors, enzyme-related systems are the most common model, and GOx underpins most of these devices.[39] Enzymatic glucose sensors use conductometric, impedimetric, potentiometric, and amperometric techniques based on GOx immobilization.[41,42] To generate an electrical connection between the electrode and enzyme, mediated electron transfer (MET) and direct electron transfer (DET) can be used. Both categories of glucose measurement sensing are based on a primary electrochemical reaction between glucose and water, which produces gluconolactone and H_2O_2 via the action of GOx. The dissociation of H_2O_2 is amplified by a small electrical current to generate free electrons, and then,

 © 2021 Wiley-VCH GmbH

Table 1. Summary of off-body nanomaterial-based optical glucose sensors.

Principle	Platform	Biological sample	LOD	Detection range	Response time	Enzyme	Refs.
Colorimetry	HRP-H_2O_2-TMB	Urine	0.03×10^{-6} M	0.2×10^{-6}–55.6×10^{-6} M	–	GOD	[26]
Colorimetry	carboxyl-NC@GOx	Urine	–	1.5×10^{-3} M–13.0×10^{-3} M	–	GOx	[15]
Colorimetry	G/H-Aerogel	Blood & sweat	11.4×10^{-6} M	–	30 min	GOx	[27]
Fluorescence	AgNPs@PCN-224	Human blood	0.078×10^{-6} M	0×10^{-3}–3×10^{-3} M	40 min	GOx	[28]
Fluorescence	CdTe QDs	Blood & saliva	5×10^{-9} M	10×10^{-9}–100×10^{-6} M	30 min	GOx	[17]
Fluorescence	GQDs/AuNCs/Fe^{2+}	Human blood	0.18×10^{-6} M	1×10^{-6}–15×10^{-6} M	15 min	GOx	[19]
Fluorescence	TP–GOx	Artificial sweat	25×10^{-6} M	25×10^{-6}–1000×10^{-6} M	45 min	GOx	[18]
NIR Fluorescence	GOx-Pt-Porphyrin-PLA-alginate hybrid	–	1.5×10^{-3} M	0×10^{-3}–10×10^{-3} M	4 min	GOx	[29]
UV-vis spectrophotometer	GOx@HP-MIL-88B-BA	Human blood	0.98×10^{-6} M	2×10^{-6}–100×10^{-6} M	10 min	GOx	[30]
Whispering gallery mode resonator	WGMRs/Au-NPs/GOx	–	–	0×10^{-3}–2.4×10^{-3} M	–	GOx	[31]
Chemiluminescence	IC/hemin/glucose/H_2O_2	Blood & urine	15.0×10^{-9} M	0.06×10^{-6}–3.5×10^{-3} M	–		[32]
Colorimetry	Gal-1 IN PEG-AuNPs	–		100×10^{-12}–10×10^{-3} M	10 min		[33]
Colorimetry	MGCN-chitin-AcOH	Blood & urine	0.055×10^{-6} M	1×10^{-6}–900×10^{-6} M	3 min		[34]
Colorimetry	MnO_2 nano-oxidizers	Human blood	10×10^{-6} M	10×10^{-6}–5×10^{-3} M	50 min		[35]
Colorimetry	NL-$MnCaO_2$	Human blood	23.86×10^{-6} M	18.3×10^{-6}–421.6×10^{-6} M	–		[13]
Colorimetry	$Pt^{2+}_{2.30}$@g-C_3N_4	–	0.01×10^{-3} M	0.13×10^{-3}–2.00×10^{-3}M	–		[21]
Colorimetry	Pd_{91}-GBLP NPs	Human blood	1×10^{-6} M	2.5×10^{-6}–700×10^{-6} M	–		[23]
Colorimetry	P-Co_3O_4	Human blood	0.69×10^{-6} M	10×10^{-6}–30×10^{-6} M	30 min		[20]
Colorimetry	R-Co_3O_4	Human blood	0.32×10^{-6} M	1×10^{-6}–20×10^{-6} M	30 min		[20]
Fluorescence	CDs/Fe_3O_4@APBA	Human blood	0.15×10^{-6} M	0.2×10^{-3}–20×10^{-3} M	5 min		[24]
Fluorescence	CNPs	Human blood	10×10^{-6} M	50×10^{-6}–2000×10^{-6} M	5 h		[16]
Fluorescence	His-AuNCs	Urine	3.4×10^{-6} M	5×10^{-6}–125×10^{-6} M	40 min		[36]
SERS	Fe_3O_4 NPs@Au NPs/d-$Ti_3C_2T_X$ MXene	Plasma	0.033 pg mL^{-1}	0.0001–100.0 ng	5 s		[37]
SERS	Ag NRs@Al_2O_3	–	$10^{-4} \times 10^{-3}$M	$10^{-3} \times 10^{-3}$–3×10^{-3} M	≈10 s		[22]
SERS	Au-ND/glucose/Ag NPs	Blood	–	1×10^{-3}–40×10^{-3} M	10 s		[25]

the glucose concentration is determined in the immediate area.[9] In terms of MET determination, voltammetry is a profitable tool that has various merits, including high sensitivity, low cost, with easy and fast sample preparation. For structural design, the working electrode plays a crucial role, and the most common electrodes are glassy carbon and mercury.[43] Therefore, numerous studies have established glassy carbon electrode (GCE)-based-sensors such as GOx/CoS-MWCNT (multi-walled carbon nanotube)/Nafion/GCE[44] and polymer phenylethnylcopper (PPhECu)-based photoelectrochemicals (PECs).[45] In particular, PEC methods have emerged as a potential analytical method with high sensitivity, low background noise, and simple equipment. The performance of PEC sensors mainly depends on photosensitive materials, and the operating principle is based on the photocurrent alteration of the electrode modified with a photoactive material. Furthermore, the PPhECu, can be synthesized, which has a high initial signal, to develop a PPhECu/GCE-based PEC device with a very low detection limit of 0.16×10^{-6} M.[45]

In order to eliminate unexpected risks, such as the instability of mediators in MET, DET application is a potential strategy and is more popular in the field of enzyme-based glucose sensors. Various studies have focused on the utilization of nanomaterials to provide high conductivities and surface areas for electrode anchoring on the surface, thus reducing the distance between the flavin adenine dinucleotide (FAD, active site of GOx) and the underlying electrode minimization in DET.[46] These nanomaterials include graphene, carbon nanotubes (CNTs), nanocomposites, nanoparticles, and conducting polymers, which are developed as micro- or nanoscale matrix/arrays, as nanomaterial-based substrates, and via layer-by-layer functionalization.[19,46] Typically, to construct GOx/MC (mesoporous carbon)-COOH bioelectrodes, GOx is immobilized on carboxylized MC before being dispersed on a carbon cloth (CC), which enhances the amount and activity of immobilized GOx, thus enriching the electrode properties.[47] The Nafion/GOx/MC-COOH platform has been shown to present good electrocatalytic activity; it not only increased the anodic charge-transfer coefficient (α) but also enhanced the peak current intensity and the reduction peak current of O_2 (**Figure 2**A).[47] In addition, various nanostructured metal oxides have a remarkable ability to facilitate electron transfer

 © 2021 Wiley-VCH GmbH

Table 2. Summary of off-body nanomaterial-based electrochemical sensors of glucose.

Type of electrode	Platform	Biological sample	Sensitivity [μA mM^{-6} cm^{-2}]	LOD	Detection range	Response time	Enzyme	Refs.
AlGaN/GaN HEMT	AuNPs/GOx	Blood	10^6	1×10^{-9} M	0.001×10^{-3}–9×10^{-3} M	< 8 s	GOx	[85]
Carbon fiber	CF-PEDOT-GOx	Blood	8.5	–	0.5×10^{-3}–15×10^{-3} M	< 2 s	GOx	[46]
Cu-nanoflowers	Cu-nanoflower@AuNPs-GO NFs	–	–	0.018×10^{-6} M	0.001×10^{-3}–0.1×10^{-3} M	–	GOx	[86]
FTO	GOx/nano-ZnO/PVA	–	41	2.0×10^{-6} M	0.2×10^{-3}–20×10^{-3} M	< 3 s	GOx	[42]
GCE	GOx/CoS-MWCNTs/Nafion	Human blood	14.96	5×10^{-6} M	8×10^{-6}–1.5×10^{-3} M	5 s	GOx	[44]
GCE	PPhECu/GCE-based PEC	Human blood	–	0.16×10^{-6} M	0.5×10^{-6}–5×10^{-3} M	–	GOx	[45]
ITO glass	3D porous graphene aerogel@GOx	Human blood	–	0.87×10^{-3} M	1×10^{-3}–18×10^{-3} M	–	GOx	[87]
Laser-induced graphene (LIG)	LIG/PtNPs/GOx	Sweat	4.622	300×10^{-9} M	0.0003×10^{-3}– 2.1×10^{-3} M	–	GOx	[88]
Pt disk	PANI-MMT/PtNPs/CS	Human blood	35.56	0.1×10^{-6} M	10×10^{-6}–1.94×10^{-3} M	–	GOx	[49]
Pt disk	Gelatin/GOx–Pt	Blood	158	0.5×10^{-6} M	0.5×10^{-6}–1.8×10^{-3} M	1.4 s	GOx	[89]
Au	AuNP-MIPs	Human blood	–	1.25×10^{-9} M	1.25×10^{-9}–2.56×10^{-6} M	–		[90]
Au	Copper-G-COOH	Human blood	1142	7.96×10^{-9} M	0.1×10^{-6}–5.48×10^{-3} M	2 s		[73]
Au	PEDOT–ERGO	Human blood	696.9	0.12×10^{-6} M	0.1×10^{-3}–100×10^{-3} M	<1 s		[91]
Carbon cloth	CuO/Ni(OH)^2	–	598.6	0.31×10^{-6} M	0.05×10^{-3}–8.50×10^{-3} M	1 s		[92]
Carbon cloth	$ZnCo_2O_4$ NWAs	Human blood	3880	2.5×10^{-6} M	5×10^{-6}–0.5×10^{-3} M	5 s		[93]
Carbon cloth	ZnO	Blood	4792	0.43×10^{-6} M	1×10^{-6}–1.45×10^{-3} M	< 3 s		[94]
Cu foam (CF)	Nanoporous Cu_2O NRs/NTs	Blood	5792.7	0.015×10^{-6}M	15×10^{-9}–0.1×10^{-6} M	< 1 s		[95]
CNF	$NiMoO_4$	Human blood	301.77	50×10^{-9} M	0.0003×10^{-3}–4.5×10^{-3} M	5 s		[96]
CF	NiCu-OH@Cu(OH)$_2$ NRA	Human blood	6560.3	32×10^{-9} M	100×10^{-9} –1.5×10^{-3} M	3 s		[68]
Cu foil	AuNPs@CuO NWs	Human blood	1591.44	0.3×10^{-6} M	0.3×10^{-6}–31.06×10^{-3} M	–		[97]
Cu foil	Cu_3Pt/Cu_2O Nanorod	Human blood	5082	1.759×10^{-6} M	0.005×10^{-3}–10×10^{-3} M	< 6 s		[62]
Cu foil	Dendritic Au	–	300	0.6×10^{-6} M	10.0×10^{-6}–15.0×10^{-3}M	–		[98]
Cu sheet	oxidized Zn–Sn hybrid nanostructures	–	2135	–	0.5×10^{-6}–0.1×10^{-3} M	1 s		[99]
Cu foil	CuS nanosheets/Cu_2O/CuO NWAs	–	4262	–	0.002×10^{-3}–4.1×10^{-3}M	–		[69]
Glassy carbon (GC)	Cu-NW-CNT-BL	–	1907	0.33×10^{-9} M	10×10^{-6}–2000×10^{-6} M	1 s		[81]
GC	Cu(OH)$_2$ particle	Blood and urine	253	–	$< 0.1 \times 10^{-3}$ M	< 4 s		[100]
GC	GC/PDPA/PTA/ZnO	–	20.30	0.1×10^{-6} M	1×10^{-6}–7×10^{-6} M	< 2 s		[56]
GC	$NiCo_2S_4$/EGF-7	Human blood	7431.96	0.167×10^{-6} M	0.0005×10^{-3}–3.571×10^{-3} M	5 s		[101]
GC	NiCP/CNTs	Human blood	2931.4	2.1×10^{-6} M	2.1×10^{-6}–400×10^{-6} M	–		[102]
GCE	AgNPs/NSC	–	35 220	0.046×10^{-3} M	5×10^{-6}–3×10^{-3} M	–		[55]
GCE	Au@NiCo LDH	–	864.7	0.028×10^{-6} M	0.005×10^{-3}–12×10^{-3}M	4 s		[52]
GCE	Au@Ni/C	–	23.17	0.0157×10^{-3} M	0.5×10^{-3}–10×10^{-3} M	3 s		[53]
GCE	AuNPs/RGO	Human sweat	–	4×10^{-6} M	10×10^{-6}–400×10^{-6} M	–		[54]
GCE	Co_3O_4	–	212.92	2.7×10^{-6} M	0.05×10^{-3}–3.2×10^{-3}M	5 s		[61]
GCE	$CoMoO_4$/MPC-2	Human blood	–	0.13×10^{-6} M	5×10^{-7}–1.08×10^{-4} M	1.76 s		[103]
GCE	Cu@C/Nafion	Human blood	2565	21.35×10^{-6} M	0.04×10^{-3}–40×10^{-3} M	–		[104]
GCE	Cu@Pd-CS	–	23.00	–	0.1×10^{-3}–1×10^{-3} M	–		[105]
GCE	Cu_2O MSs/S-MWCNTs	Human blood	581.89	1.46×10^{-6} M	0.00495×10^{-3}–7×10^{-3} M	–		[59]
GCE	CuO-350-AIR	Saliva	1806.1	0.15×10^{-6} M	5×10^{-6}–1.165×10^{-3} M	3 s		[106]
GCE	$Cu_3(BTC)_2$-derived CuO nanorod	–	1523.5	1×10^{-6} M	1×10^{-6}–1.25×10^{-3} M	5 s		[107]
GCE	Cu-$x$$Cu_2O$ NPs@3DG foam	–	230.86	16×10^{-6} M	0.8×10^{-3}–10×10^{-3} M	–		[41]
GCE	Cu@HHNs	Human blood	1594.2	1.97×10^{-6} M	5×10^{-6}–3×10^{-3} M	–		[84]
GCE	E-NiCo-BTC	Human blood	230.5	0.187×10^{-6} M	0.0×10^{-3}–5.7×10^{-3} M	–		[63]
GCE	rGO-Cu_2O micro-octahedrals (without Nafion)	Human blood	24.8	0.53×10^{-6} M	1×10^{-6}–9000×10^{-6} M	–		[58]

 © 2021 Wiley-VCH GmbH

Table 2. Continued.

Type of electrode	Platform	Biological sample	Sensitivity [μA mM^{-6} cm^{-2}]	LOD	Detection range	Response time	Enzyme	Refs.
GCE	rGO-Cu_2O micro-octahedrals (with Nafion)	Human blood	415	0.96×10^{-6} M	1×10^{-6}–9000×10^{-6} M	–		[58]
GCE	*n*CuO-MHS/Nafion	–	25.46	1×10^{-6} M	0.001×10^{-3}–3×10^{-3} M	–		[108]
GCE	Ni@Cu-MOF	Human blood	1703.33	1.67×10^{-6} M	5×10^{-6}–2500×10^{-6} M	–		[82]
GCE	$NiFe_2O_4$-NiCo-LDH@rGO	Human blood	111.86	12.94×10^{-6} M	3.5×10^{-5}–4.525×10^{-3} M			[64]
GCE	Ni-MOF400	Bovine serum	2918.2	0.92×10^{-6} M	5×10^{-6}–4.1×10^{-3} M	–		[83]
GCE	NiO-NC-rGO	Human blood	4254	70.9×10^{-9} M	0.5×10^{-6}–20.0×10^{-6} M	–		[109]
GCE	NiO nanodonuts	–	904.6	1.4×10^{-6} M	0.05×10^{-3}–9.5×10^{-3} M	2 s		[60]
GCE	Ni_5P_4	Human blood	149.6	0.7×10^{-6} M	0.002×10^{-3}–5.3×10^{-3} M	–		[50]
GCE	Pd–Ni@f-MWCNT	Human blood	71	0.026×10^{-6} M	0.01×10^{-3}–1.4×10^{-3} M	3–5 s		[66]
GCE	PtAu	Human blood	–	3×10^{-6} M	0.01×10^{-3}–10×10^{-3} M	–		[65]
GCE	ZnO/CeO_2	–	–	0.224×10^{-6} M	0.5×10^{-6}–300×10^{-6} M	–		[110]
Graphene	Ni-G-PLA	Blood and saliva	–	2.4 μmol L^{-1}	2.0–20.0 in blood 0.02–0.20 in saliva	–		[111]
FTO	CuO	–	1207	1.19×10^{-6} M	1.19×10^{-6}–2.2×10^{-3} M	< 4 s		[112]
FTO	Fe_2O_3NR	–	100.46	5.5×10^{-6} M	0.5×10^{-3}–2.5×10^{-3} M	–		[113]
FTO	PdNS-Cu/Cu_2O	Human blood		0.1×10^{-6} M	0.5×10^{-6}– 2600×10^{-6} M	5 s		[67]
ITO	Au-NiO_{1-x}HNAs	Human blood	4061	0.001×10^{-3} M	0.005×10^{-3}–15×10^{-3} M	–		[114]
ITO	CuO PNBs	Human blood	1876.52	60×10^{-9} M	0.1×10^{-6}–2×10^{-3} M	–		[78]
ITO	Hybrid Cu_2O-ZnO	Blood	441.2	0.13	0.02×10^{-3}–1×10^{-3} M	< 3 s		[57]
ITO	LI–NiEC–CdS–G	–	–	0.4×10^{-6} M	1.0×10^{-6}–1.0×10^{-3} M	–		[115]
ITO	NiNPs/ERGO	–	185 200	40×10^{-9} M	0.5×10^{-6}–244×10^{-6} M	4 s		[116]
ITO	Pd-PBTh	–	5620	7×10^{-6} M	0.04×10^{-3}–0.4×10^{-3} M	3 s		[79]
MEM	MWCNTs-TBA-MIPs/AFC/MEM	Blood	–	0.61×10^{-6} M	1×10^{-6}–180×10^{-6} M	–		[117]
Ni film	Ni/Cu bowl-like array film	Urine	3924	0.05×10^{-6} M	0.5×10^{-6}–2.5×10^{-3} M	5 s		[74]
Ni foam	Ag@CNC@NF	–	3.64×10^{10}	6×10^{-9} M	0.5×10^{-3}–7×10^{-3} M	0.1 s		[51]
Ni foam	ND-Gr-NH	Human blood	15431.2	0.1×10^{-6} M	5×10^{-6}–2000×10^{-6} M	1 s		[72]
Ni foil	GLAD Ni thin film	Urine and sweat	1600	0.05×10^{-6} M	0.5×10^{-6}–9×10^{-3} M	–		[70]
Ni foil	GLAD NiO thin film	Urine and sweat	4400	0.007×10^{-6} M	0.5×10^{-6}–9×10^{-3} M	–		[70]
Ni foil	$NiMn_2O_4$ NSs@NF	–	12 300	0.24×10^{-6} M	0.115×10^{-3}–0.661×10^{-3} M	2 s		[71]
Ni substrate	$Cu_xCo_{3-x}O_4$ nanoneedle framework thin-film	–	13 291.7	1.36×10^{-6} M	Up to 1.4×10^{-3} M	< 0.5 s		[118]
Platinum foil	$Ni_{60}Nb_{40}$ nanoglass	–	20 000	100×10^{-9} M	2×10^{-3}–38×10^{-3} M	–		[119]
Polyurethane (PU)	$Ni(OH)_2$/PU	–	2845	0.32×10^{-6} M	0.01×10^{-3}–2.06×10^{-3} M	< 5 s		[120]
Porous CuO	CuO PN	Saliva	2299	0.41×10^{-6} M	5×10^{-6}–0.225×10^{-3} M	0.8 s		[121]
Pt	$Co_xO_yH_z$@ZIF-67/TiO_2 NTs	Human blood	–	0.03×10^{-6} M	0.1×10^{-6}–1×10^{-3} M	–		[122]
Titanium foils	BiOBr-TNTA	Human blood	773	10×10^{-9} M	$(5 \times 10^2) \times 10^{-9}$–$(3 \times 10^7) \times 10^{-9}$ M	–		[75]
Titanium foils	NiCo/TiO_2@C NFAs	Human blood	975.3	0.6×10^{-6} M	1×10^{-6}–7658×10^{-6} M	5 s		[123]
LIG	Cu NPs	Blood	495	0.39×10^{-6} M	1×10^{-6}–6.0×10^{-3} M	0.5 s		[124]

between the active surface site and the electrode.[42] In a recent study, GOx was immobilized on a ZnO–polyvinyl alcohol (PVA) composite film before being deposited on fluorinated tin oxide (FTO) using a spin-coating technique to construct a voltammetric sensor—GOx/nano-ZnO/PVA/FTO. This sensing platform not only responds quickly (less than 3 s) but also reaches a high sensitivity of 0.041 mA mM^{-1} to detect glucose in real human blood serum samples.[42] Additionally, platinum electrodes have been increasingly used to generate a working electrode with high reproducibility and stability, based on the very low and stable baseline current of the Pt electrode.[48] Recently, in one study, a novel amperometric sensor was developed by

© 2021 Wiley-VCH GmbH

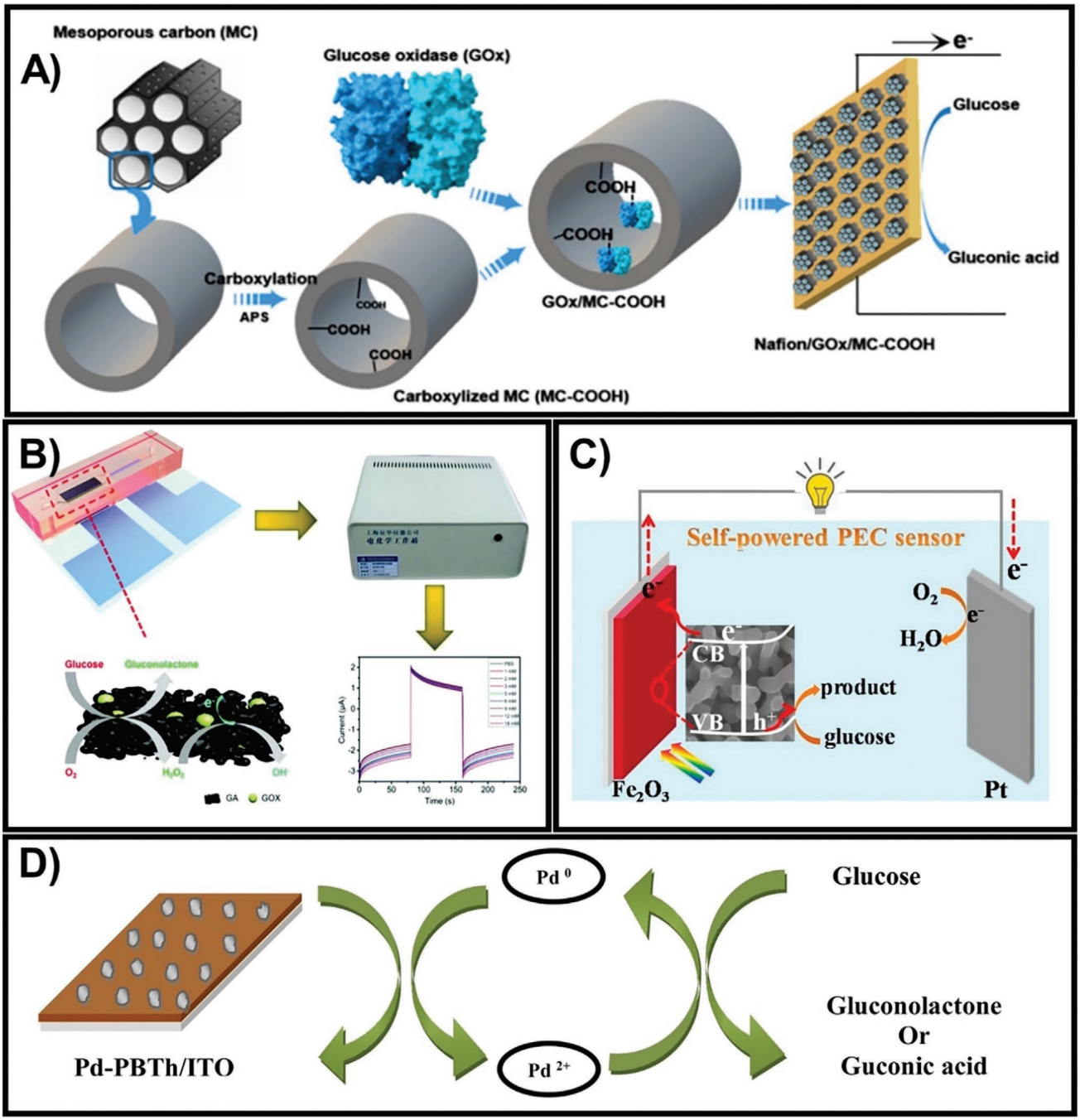

Figure 2. A) Fabrication of the Nafion/GOx/MC-COOH sensor by dispersing GOx-immobilized MC/COOH onto a carbon cloth electrode. Adapted with permission.[47] Copyright 2020, MDPI. B) The fundamental principle of the 3D porous graphene aerogel@GOx system as a microfluidic biosensor. Adapted with permission.[87] Copyright 2020, Royal Society of Chemistry. C) The PEC self-powered sensor was constructed using a Fe_2O_3NR photoanode and platinum wire cathode. Adapted with permission.[77] Copyright 2020, Elsevier. D) The mechanism of enzyme-free electrochemical platform Pd-PBTh/ITO. Adapted with permission.[79] Copyright 2020, Elsevier.

electrodepositing Pt nanoparticles (PtNPs) on polyaniline montmorillonite (PANI-MMT) hybrid nanocomposite and then immobilizing it on glucose oxidase (GOD), resulting in the fabrication of a PANI-MMT/PtNPs/CS-GOD sensor. This developed sensor exhibited a quick response in determining human blood serum glucose levels with a high sensitivity of 35.56 μA mM^{-1} cm^{-2} and limit of detection (LOD) of 0.1×10^{-6} M.[49] Although they guarantee glucose detection because of the high sensitivity and good selectivity,[19] these sensing platforms have several drawbacks similar to optical devices, as mentioned in a previous study.[41] Therefore, to tackle these issues of enzymatic-related sensors, 3D porous graphene aerogels in microfluidic systems have been established as novel amperometric sensors. This platform exhibits some considerable merits,

© 2021 Wiley-VCH GmbH

including increased specific surface area, which can be used to modify more GOx, enhanced physiological conditions, and limited contamination of GOx. Because of these factors, a sensor with good biocompatibility, low sample consumption, long-term enzyme activity, and stability for practical use was developed (Figure 2B).[87]

2.2.2. Novel Investigation of Enzyme-Free Electrochemical Glucose Sensors

Alternatively, the development of enzyme-free devices to overcome the challenges of enzymatic-glucose probes has attracted attention, to develop probes with advantages such as low cost, fast response, good sensitivity, ultra-low detection limit, and long-term stability.[50,51] Currently, among the numerous cutting-edge technological devices, especially in terms of glucose sensors, GCE has numerous attractive properties such as a low background current and convenient fabrication; therefore, it is an important electrode for nonenzymatic instruments. However, a drawback of this platform is its slow electron transfer; thus, it is necessary to modify the surface of the electrode by loading it with various catalyst nanomaterials such as noble and transition metal/metal oxides (e.g., Au,[52–54] Ag[55]/ZnO,[56,57] Cu_2O,[58,59] NiO,[27,60] and Co_3O_4[61]) and alloys/complexes (e.g., Cu_3Pt,[62] Ni_5P_4,[50] and NiCo[63,64]).

Both noble metals (e.g., Au, Ag, Pt,[65] and Pd[66,67]) and transition metals (e.g., Cu[68,69] and Ni[70–72]) ameliorate glucose oxidation in an electrocatalytic manner; thus, they are commonly employed for glucose quantification. In particular, noble metals possess essential electrocatalytic activity; thus, in the last few years, they have been intensely applied in nonenzymatic glucose platforms.[69] In particular, a conifer-like copper-G-COOH nanocomposite was prepared and then deposited on a bare gold electrode to fabricate an enzyme-free glucose sensor with high sensitivity, low LOD, and fast response of under 2 s.[73]

Nonetheless, metal nanoparticles are expensive and susceptible to poisoning, which minimizes their wide application. Fortunately, several alternative investigations have attempted to tackle these problems by combining nanoparticles with transition metals or transition metal oxides.[73] For instance, copper foil or copper oxide (Cu_2O or CuO) has been used to successfully construct electrochemical glucose sensors because of their high isoelectric point and low overpotential for electron-transfer reactions.[71] Based on a simple and easy synthesis technique, a copper foil can be grown into various CuO nanostructures such as nanoflowers, nanowires, and nanorods, which have many advantages.[74] Li et al. developed CuO nanowires (NWs) on 3D copper foam followed by coating gold nanoparticles (Au NPs) to form CuO NWs with Au NPs.[74] Cu_3Pt/Cu_2O nanorod arrays with different CuO nanostructures were synthesized by Yang et al. using the immersion-reduction method. Note that this sensor has a large surface area for glucose contact and a fast electron transfer path; thus, it exhibits an outstanding sensitivity of 5082 $\mu A\ mM^{-1}\ cm^{-2}$ and a fast response time (<6 s).[73] Nickel (Ni), which is also an excellent material, possesses excellent sensitivity, stability, and outstanding ability to catalyze glucose oxidation in alkaline media and is widely applied in sensors.[70,74] Zhang et al. developed a novel nonenzymatic glucose sensor of porous $NiMn_2O_4$ NS@NF via a hydrothermal method followed by heat treatment. This sensor responds quickly (within 2 s) and has a very high sensitivity of 12.3 $mA\ mM^{-1}\ cm^{-2}$ for glucose.[71] Human serum is used as the sample for almost all conventional glucometers, which is extracted via invasive methods, leading to discomfort and pain for the patients. Therefore, it is necessary to investigate noninvasive glucose sensors using other biological fluids such as urine, sweat, and saliva.[39] For instance, Singer et al. fabricated two amperometric electrochemical integrated devices using Ni and NiO electrodes, which were fabricated via the glancing angle deposition (GLAD) technique. Although they were utilized to quantify glucose in artificial sweat and urine samples, the GLAD NiO thin film platform was better than the GLAD Ni thin film in terms of sensitivity and LOD.[70] Additionally, TiO_2 has exceptional photosensitivity and chemical stability; thus, it is possible to apply it as an electrode in PEC devices.[75] Moreover, to enhance the electrocatalytic performance, free-standing 1D nanostructures have been established as direct pathways for electron transport and binder-free contact with the electrocatalyst.[75] In particular, the performance of the BiOBr–TiO_2 nanocomposites was confirmed by Zhao et al., which showed good photocatalytic activity, excellent stability, and high photocurrent densities under visible light conditions. Hence, the fabricated BiOBr-TNTA sensors via vacuum impregnation and chemical precipitation achieved a minimum LOD of 10×10^{-9} M.[75]

Among the three principal categories of transparent conductive oxide (TCO) films, SnO_2-based films have enormous potential, including high hardness, low electrical resistivity, good electrochemical stability, high optical transmittance, and especially, the large amount of tin resources. Nevertheless, SnO_2, the natural semiconductor, is a nonconductive material. Various doping elements (e.g., Mn, Sb, and F) have been applied to modify the crystal structure of SnO_2 thin films by various coating techniques such as chemical vapor deposition, spray pyrolysis, or sol–gel methods to synthesize fluorine-doped tin oxide (FTO) films.[76] He et al. utilized FTO films and hematite (Fe_2O_3) nanorod (NR) structures to fabricate an Fe_2O_3NR/FTO electrochemical glucose sensor (Figure 2C).[77] Because of the inherent advantages of Fe_2O_3 such as abundance, eco-friendliness, nontoxicity, good light absorption, and especially, photochemical stability in alkaline electrolytes, the electricity required for this system could be obtained from renewable solar energy, and the glucose-monitoring device could be self-powered. Another application that utilizes the rich source of tin is indium tin oxide (ITO) electrode, which exhibits robust sensing stability.[78] In particular, the ITO electrode was modified by electropolymerization of bithiophene to form PBTh/ITO, followed by the electrodeposition of palladium particles onto the PBTh/ITO film, and the construction of an amperometric Pd-PBTh/ITO glucose sensor (Figure 2D). This proposed platform responded quickly within ≈3 s with exceptional sensitivity of ≈5620 $\mu A\ mM^{-1}\ cm^{-2}$.[79]

Additionally, various carbon-based materials have been synthesized as supports for loading metal-based substances or nanocomposites, such as graphene or graphene oxide (GO), CNTs, and other carbon substances.[38] Graphene is a single graphite sheet and exhibits unique electronic, mechanical, and

© 2021 Wiley-VCH GmbH

optical properties. Its electrocatalytic properties can be improved by depositing heteroatoms (e.g., N, B, P, and S).[80] Typically, GCE/rGO-Cu_2O micro-octahedrals, which is a differential pulse voltammetry electrical glucose sensor, was investigated hydrothermally to detect glucose levels in human serum. For the first time, the utilization of ascorbic acid has led to easy accumulation of Cu_2O onto the reduced GO (rGO) to form rGO-Cu_2O micro-octahedrals before attaching to the GCE.[58] In contrast, Palve et al. recently applied CNTs to develop an amperometric Cu-NW-CNT-BL/GCE glucose sensor. First, copper nanowires (Cu-NWs) were synthesized via an ethylenediamine-mediated method. Then, Cu-NW and CNT were loaded on GCE by layer-by-layer film deposition. This platform could respond quickly in 1 s and could detect glucose at a minimum level of 0.33×10^{-9} M.[81] Furthermore, another CNT modification, MWCNTs, have also been employed for efficient electrochemical sensor applications.[59,66] Typically, functionalized MWCNTs are combined using several procedures, such as side splitters, which act as fundamental components in the construction of Pd–Ni@f-MWCNT.[66] Recently, numerous metal-organic framework (MOF) materials have emerged as a promising component for nonenzymatic glucose sensor production. However, in the electrochemical platform, they experienced a serious deficiency, which is low conductivity. Thus, they are commonly used in the derivative form. Alternatively, various conductive materials, such as noble metal nanoparticles, CNTs, or graphene, have been integrated to improve the conductivity of MOFs.[82] To concretize these development potentials, several remarkable achievements have been reported: Ni-MOF400/GCE by Yin et al.,[83] Ni@Cu-MOF/GCE by Xue et al.,[82] or ZIF-8, a zeolite-type metal-organic framework to form hydrophilic hierarchically porous nanoflowers (HHNs) and finally construct Cu@HHN sensors, by Zhu et al.[84]

Intriguingly, in recent reports, the electrochemical glucose-monitoring system has demonstrated the possibility of highly sensitive quantifiable acquisition as well as low LOD within a short time. Collectively, the various advantages offered by electrochemical devices, as already mentioned, have recently broadened new avenues toward the commercialization of glucose monitoring for diabetes.

Indeed, over 30% of COVID-19 infected patients suffered underlying disease which most of them had diabetes and hypertension.[125] Various studies indicated that it is hard to comprehensive treatment for diabetes patient suffering viral infection due to fluctuations of their blood glucose levels, cause complications and mortality increase.[4,126] Applying remotely blood glucose evaluation for not only severe COVID-19 patients but also inpatients, facilitates proper glycemic control, minimization of hospitalizations as well as invasive procedures.[126–128] Therefore, during the on-going COVID-19 pandemic, continuous glucose self-management is an urgent requirement for better diabetes care under severe quarantine to make adequate intervention for patient and reduce the risk of exposure to medical staff.[4] More importantly, the off-body glucose sensors could serve as confirming test for patients with diabetes. Hence, to overcome these difficult circumstances, an urgent request should be implemented for novel sensing with higher accuracy and feasibility of the intervention for diabetes patients without hospital admission.

3. Emergence of On-Body Wearable Glucose Continuous Monitoring

For glucose monitoring, blood is the most exploited biofluid because of the abundance of glucose. However, direct blood glucose measurement requires an in-hospital invasive sampling, which is considered as a significant risk factor contributing to the spread of coronavirus. Furthermore, the recent studies have reported the increased severity of COVID-19 disease in patients with diabetes with ≈2.85-fold of death higher than those without diabetes.[129,130] Therefore, it is the crucial necessity to shift from direct communication to remote glucose monitoring to control glucose level in individuals, minimizing the severe effects of COVID-19. Owing to their noninvasive access, external biofluids, including sweat, interstitial fluid (ISF), saliva, and tears, are desirable alternatives to blood for the monitoring of various biological analytes, including glucose.[131–134] In the past few years, efforts have been made to develop wearable sensing devices for continuous, noninvasive detection of glucose levels in these alternative body fluids, which have helped address the key drawbacks of blood glucose monitoring. Due to excellent properties of nanomaterials, nanoscale materials have been employed in wearable CGM sensor fabrication to improve sensing performance. Besides, several nanomaterial-free platforms have also shown their excellent sensing performance for glucose level with good comfort for the wearers. Herein, we summarize the most recently developed wearable sensing devices for on-body continuous measurement of glucose levels in specific biofluids (**Table 3**) and highlight the state-of-the-art methods of this field. We further discuss the advantages and drawbacks of each biofluid source involved in designing glucose wearable sensing devices.

3.1. Sweat-Based Glucose Monitoring

Among the common body fluids, sweat is the most widely exploited for target analyte determination because of its ease of collection, noninvasive accessibility, and rich physiological information.[174–176] Furthermore, sweat can be easily and continuously generated either during exercise or by on-demand stimulation with cholinergic drugs, making it a readily accessible biofluid for continuous monitoring of glucose level during daily activity. The wide distribution of sweat glands over the body makes it suitable for the rapid monitoring of glucose after device integration. In the context of hyperglycemia and diabetes, the ease of access has led to massive development toward the utilization of sweat-based wearable platforms for glucose sensing.[177–180] Sweat can be easily sampled at the skin surface within several minutes by simply attaching the sensing device containing a sweat collector to the epidermal area, that allows immediate measurement. Various remote devices for glucose monitoring have been developed, including temporary tattoos,[181] patches,[145,182] wrist bands,[183] microfluidic devices,[135,136,153] and textile-based wearable systems.[140,160,184] Owing to advancement of materials, fabrication techniques, and sampling approaches, a number of skin-interfaced biosensors have been validated for their real-time CGM in sweat during physiological activities (**Figure 3**).[135–161,185] Electrochemical sensors are the most commonly used method

© 2021 Wiley-VCH GmbH

Table 3. Summary of wearable glucose-sensing platforms with specifications regarding the type of biofluids and devices.

Platform	Analytical technique	Nanocomposite	Recognition element	Signal transition method	Biofluid	Response time	LOD	Detection range	Sensitivity	Refs.
Chip	Colorimetry	–	GOx	Image processing	Sweat	15 min	0.03×10^{-3} M	0.1×10^{-3}–0.5×10^{-3} M	–	[135]
Cotton thread	Colorimetry	–	GOx	Digital image processing	Sweat	60 s	35×10^{-6} M	50×10^{-6}–250×10^{-6} M	0.19 μM^{-1}	[136]
Cotton thread	Colorimetry	CNF/Chitosan	GOx	Image processing	Sweat	-	0.1×10^{-3} M	0.1×10^{-3}–3×10^{-3} M	–	[137]
Patch	Colorimetry	–	GOx	Image processing	Sweat	-	-	50×10^{-6}–300×10^{-6} M	–	[138]
Silicone elastomers	Colorimetry	–	GOx	Image processing	Sweat	1 min	-	4×10^{-6}–40.4×10^{-6} M	–	[139]
Textile/paper	Colorimetry	PU@Chitosan	GOx	Color converting program	Sweat	–	13.49×10^{-6} M	50×10^{-6}–600×10^{-6} M	–	[140]
Patch	Fluorescence	–	GOx	Image processing	Sweat		7×10^{-6} M	10×10^{-6}–250×10^{-6} M		[141]
Smartwatch	Photoplethysmogram	–	–	Bluetooth	Sweat	–	–	50–350 mg dL^{-1}	–	[142]
Skin pad	Ratiometric fluorescence	BiM-CQDs@PSi	GOx	Image processing	Sweat	–	–	–	3.46% mM^{-1}	[143]
Electronic skin	Electrochemical	MDB@TTF@ CNT@rGO@h-Ni	GOx	Bluetooth	Sweat	–	–	0×10^{-6}–150×10^{-6} M	0.1 mV μM^{-1}	[144]
Epidermal patch	Electrochemical	PB@Chi@Nafion	GOx	Bluetooth	Sweat	4–7 s	–	10×10^{-6}–200×10^{-6} M	–	[145]
Film	Electrochemical	$NiCo_2O_4$/Chitosan	-	WiFi	Sweat		10×10^{-6} M	10×10^{-6} to 200×10^{-6} M	0.5 $\mu A\ \mu M^{-1}$	[146]
Film	Electrochemical	PI@PMMA@APTES@ SWCNT@Nafion	GOx	Bluetooth	Sweat	5 s	50×10^{-6} M	50×10^{-6}–1×10^{-3}M	41.397 μM^{-1}	[147]
Film	Electrochemical	CNT-EVA	GOx		Sweat	3 s	3×10^{-6} M	–	270 ± 10 $\mu A\ mM^{-1}\ cm^{-2}$	[148]
Gloves	Electrochemical	BGNPs	GOx	Bluetooth	Sweat	60 s	11.6×10^{-6} M	0×10^{-3}–2.1×10^{-3} M	20.22 μA $mM^{-1}\ cm^{-2}$	[149]
Patch	Electrochemical	NPG	–	PStouch Android	Sweat	–	–	0.01×10^{-3}–1×10^{-3} M	253.4 $\mu A\ cm^{-2}\ mM^{-1}$	[150]
Patch	Electrochemical	WSNFs@Au@rGO@PU	–	PStouch-PalmSens	Sweat	–	500 $\times 10^{-9}$ M	0.5×10^{-9}–1×10^{-3} M	140 $\mu A\ mM^{-1}\ cm^{-2}$	[151]
Patch	Electrochemical	HA–AuNP	GOx	Wireless	Sweat	5 s	0.5 mg dL^{-1}	0.5–50 mg dL^{-1}	12.37 $\mu A\ dL\ mg^{-1}\ cm^{-2}$	[152]
Patch	Electrochemical	PB@Graphite@Nafion	GOx	–	Sweat	–	5×10^{-6} M	0×10^{-3}–1.9×10^{-3} M	35.7 $\mu A\ mM^{-1}\ cm^{-2}$	[153]
Patch	Electrochemical	PET@Au@PB	GOx	–	Sweat	1 min	–	50×10^{-6}–200×10^{-6} M	1.0 nA μM^{-1}	[154]
Patch	Electrochemical	CNTs/Ti3C2Tx/PB/CFMs	GOx	Bluetooth	Sweat	30 s	0.33 × 10–6 M	10×10^{-6}–1.5×10^{-3} M	35.3 $\mu A\ mm^{-1}\ cm^{-2}$	[155]
Patch	Electrochemical	PEDOT:PSS@ PLL-*g*-OEG4-biotin	GOx	Microwave	Sweat	-	0.1×10^{-9} M	0.1×10^{-9} M-10×10^{-3} M	0.026 dB/log ($\times 10^{-9}$ M)	[156]
Smartwatch	Electrochemical	Zn-MnO_2	GOx	Analog-to-digital port	Sweat	–	–	50×10^{-6}–200×10^{-6} M	3.29 nA μM^{-1}	[157]
Sweatband	Electrochemical	Pd@ZIF-67	–	Bluetooth	Sweat	27 s	2.0×10^{-6} M	–	–	[158]
Textile bands	Electrochemical	PU@SWCNT@PB	GOx	–	Sweat	–	–	–	8 nA μM^{-1}	[159]
Textile patch	Electrochemical	SilkNCT	GOx	Bluetooth	Sweat	–	5×10^{-6} M	25×10^{-6}–300×10^{-6} M	6.3 nA μM–1	[160]
Wearable device	Electrochemical	Au@PI@TTF@ CNT#Nafion	GOx	Bluetooth	Sweat	–	–	–	–	[161]

© 2021 Wiley-VCH GmbH

Table 3. Summary of wearable glucose-sensing platforms with specifications regarding the type of biofluids and devices.

Platform	Analytical technique	Nanocomposite	Recognition element	Signal transition method	Biofluid	Response time	LOD	Detection range	Sensitivity	Refs.
Package	Colorimetry	–	GOx	Bluetooth	ISF	3 s	68×10^{-6} M	0×10^{-3}–8×10^{-3} M	0.026 ± 0.002 mM^{-1}	[162]
Smartwatch	VIS-NIR	–	–	LED	ISF	–	–	70–152 mg dL^{-1}	–	[163]
Microneedle	Electrochemical	pMB/Au-MWCNTs	FAD glucose hydrogenase	Bipotentiostat	ISF	120 s	7×10^{-6} M	0.05×10^{-3}–5×10^{-3} M	405.2 ± 24.1 μA cm^{-2} mM^{-1}	[164]
Patch	Electrochemical	PB@CA@β-CD NF	GOx	–	ISF	3 s	9.35×10^{-5} M	0.1×10^{-3}–5×10^{-3} M	5.08 μA mM^{-1}	[165]
Slot antenna	Electromagnetism	–	–	Microwave	ISF	–	10 mg dL^{-1}	10–600 mg dL^{-1}	–	[166]
Smartwatch	Electromagnetism	–	–	Medtronic Zephyr BioPatch	ISF	5 min	3.8 mmol L^{-1}	4–7.5 mmol L^{-1}	–	[167]
Paper strip	Colorimetry	–	GOx	LED light RGB color sensor	Saliva	5 s	32 mg dL^{-1}	32–516 mg dL^{-1}	1.0 mg dL^{-1}	[168]
Mouthguard	Colorimetry	–	GOx	Image processing	Saliva	40 s	27 μmol L^{-1}	0–2.0 mmol L^{-1}	50.29 AU (mmol L^{-1})$^{-1}$	[169]
Infant pacifier	Electrochemical	PET/PB	GOx	Bluetooth	Saliva	–	0.04×10^{-3} M	0.1×10^{-3}–1.4×10^{-3} M	0.69 ± 0.04 nA mM^{-1}	[170]
Smart toothbrush	Electrochemical	–	–	Bluetooth	Saliva	5 s	6.6×10^{-6} M	0×10^{-6}–320×10^{-6} M	480 μA mM^{-1} cm^{-2}	[171]
Contact lens capacitor	Electrochemical	IOC-SiO_2-PtNFs	GOx	–	Tear	4 s	0.012×10^{-3} M	1×10^{-3}–20×10^{-3} M	–	[172]
Eyeglass	Microfluidic electrochemical	PB	GOx	Bluetooth	Tear	15 min	–	–	–	[173]

for wearable device design owing to their high sensitivity and simplicity, low-cost fabrication, high speed, and high analytical performance.[186–188] Several strategies have been developed to optimize the on-body sensing capability of these wearable electrochemical sensors. A sweatband-based flexible printed circuit board (FPCB)-connecting MOF as a nonenzymatic sensor was integrated for real-time analysis of sweat glucose.[158] The fabrication process is illustrated in Figure 3A. The sensor was fabricated using Pd nanoparticles (Pb NPs) enveloped in a Co-based zeolitic imidazole framework (ZIF-67) (Pd@ZIF-67) based on the water-splitting electrocatalytic property. This sensor platform was then connected to an FPCB, followed by a connection from a Bluetooth low-energy chipset to an Android-based smartphone app that enables real-time detection of body glucose. The increasing pH caused by proton reduction allowed this device to detect glucose under biological pH with no added reagents, allowing maintenance-free and long-time monitoring of glucose. The as-fabricated wearable sensing device exhibited a low LOD of 2×10^{-6} M after a 27 s response time and exhibited a good correlation with the blood glucose concentrations determined by a commercial glucometer on the same participants. This exceptional performance demonstrated the efficiency and reliability of the sweatband sensor for noninvasive clinical analysis of glucose detection and application during daily activities. To improve the sensing sensitivity and device flexibility during user activity, another electrochemical sensor utilizing an ethylene-vinyl acetate copolymer (EVA)-meso/macroporous CNT nanocomposite was proposed[148] (Figure 3B). The sensor was fabricated based on a horseradish peroxidase (HRP)-coupled glucose oxidase (GOx) mediator-free system. The productive orientation of the enzymes was enhanced through immobilization on the hierarchical meso/macroporous CNT, which enabled direct electron transfer, leading to the improvement of the sensor's sensitivity. Such sensing components were integrated into a flexible, wearable film for on-body monitoring of sweat glucose during exercise. This device presented one of the highest sensitivities for glucose detection to date with an LOD of 3×10^{-6} M and fast response of 3 s. It also showed high stability after a 7 day storage period under 4 °C and high sensitivity for the selective detection of glucose in the presence of other common interferences in sweat. The real-time applicability of the sensor was also demonstrated on volunteer participants, implying the reliability of the sensor for CGM.[148] To improve the feasibility of the sensing device, the power generation efficacy is considered. Due to their suitable power generation properties, biofuel cells have been recently fabricated in the form of electronic skin for glucose sensing in situ through wireless transmission via Bluetooth communication.[144] The unique feature of this device is the integration of 0D to 3D nanomaterials, which results in high power intensity, allowing long-term stable performance. Finally, sweat glucose levels were detected upon glucose oxidation reaction caused by GOx (Figure 3C). The as-prepared sensor showed a linear response of glucose concentration in a physiologically correlated range from 0 to 150×10^{-6} M and a sensitivity of 0.1 mV μM^{-1}. The long-term electrochemical stability of the sensor indicated its potential for continuous wearable use. Another important property of this sensing device is the combination of two types of sensors and a microfluidic module on soft e-skin; thus, this wearable device represents a combinatorial

 © 2021 Wiley-VCH GmbH

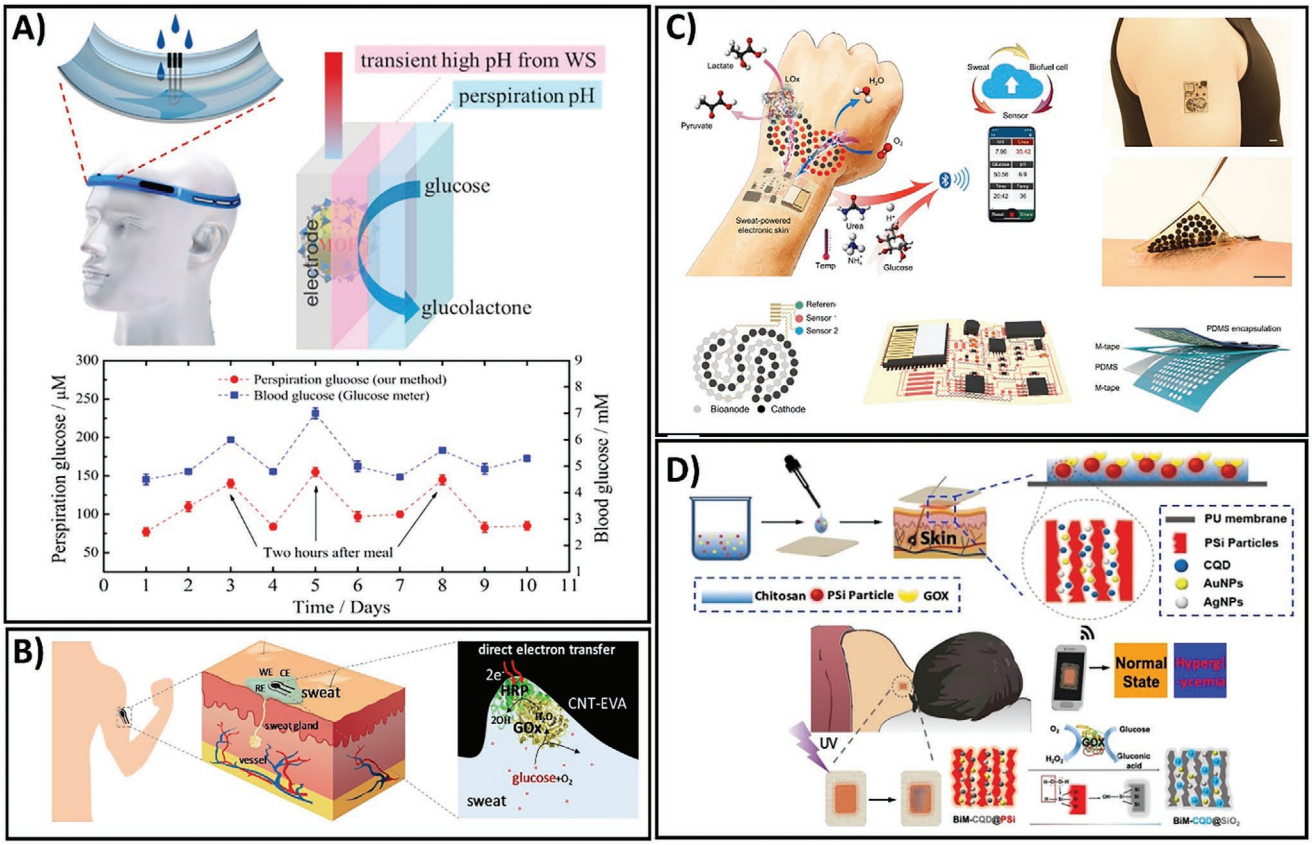

Figure 3. A) High correlation between blood glucose level and sweat glucose concentration measured using a commercial glucometer and water splitting-assisted electrocatalysis-based sweatband sensor, respectively. Adapted with permission.[158] Copyright 2019, American Chemical Society. B) The procedure of mediator-free wearable electrochemical biosensors for sweat glucose monitoring based on the bienzyme system via direct electron transfer reaction. Adapted with permission.[148] Copyright 2020, Elsevier. C) The preparation and detection processes of battery-free, biofuel-powered soft electronic skin for glucose wireless sensing. Adapted with permission.[144] Copyright 2020, The American Association for the Advancement of Science. D) Fabrication and monitoring procedure of a BiM-CQD@PSi-based enzymatic sensing device for noninvasive and visual monitoring of sweat glucose. Adapted with permission.[143] Copyright 2020, American Chemical Society

platform that provides highly improved reliability of sensing results for on-body monitoring. As such, the on-body validation showed a minor delay for continuous monitoring with an invariable performance after 60 h continuous monitoring. Furthermore, during the biking process, the glucose level in sweat detected by this sensor decreased quickly and then remained constant over time, which was well correlated with the physiological glucose levels, indicating its stability and reusability during long-term operation. Such good fabrication properties make this compact e-skin format a successful alternative to solve the problems of on-board interaction of low-energy Bluetooth, providing a tool for tremendous robotic and wearable healthcare possibilities. Although electrochemical sensors are still being developed for more accurate and comfortable wearable platforms, ratiometric fluorescence-based sensors have attracted increasing attention in the last 2 years owing to their prominent photoluminescence.[189,190] A promising example of such ratiometric fluorescence-based sensing platforms for sweat glucose monitoring was recently reported.[143] Figure 3D illustrates the construction process of a ratiometric fluorescent nanohybrid-based wearable skin pad for the noninvasive and remote control of sweat glucose. To elevate the fluorescence and oxidation kinetics of PSi and thus enhance the detection sensitivity, bimetallic (Ag and Au) nanoparticles (BiM) were doped on the luminescence porous silicon (Psi) particles (BiM@PSi). For fabricating a dual fluorescent nanohybrid, BiM@PSi particles were entrapped on carbon quantum dots (CQDs) to form a CQD/BiM@PSi composite. The as-prepared nanocomposite was then co-immobilized with GOx into a wearable skin pad, which can be attached on the body; then, under the oxidation of sweat glucose by GOx, H_2O_2 is generated, leading to a change in the ratiometric fluorescence from red to blue in a manner proportional to the sweat glucose level. Owing to the excellent properties of the BiMCQD@PSi/GOX/CS/PU pad, the resultant sensor presented a fast ratiometric fluorescence change with increased sensitivity, which was easily captured and analyzed by a camera on a smartphone. The platform was successfully employed for noninvasive and visible detection of glucose levels in diabetes/healthy volunteers during night sleep and showed clear resolution between normal glucose and hyperglycemic levels. Furthermore, the results obtained by this wearable pad agree with those obtained using a marketed blood glucometer, revealing its reliability and applicability for noninvasive tracking of the physiological state. The accurate, sensitive, and timely detection of sweat glucose level enables real-time monitoring of human daily healthcare management in an easy, simple, yet effective and robust method.

© 2021 Wiley-VCH GmbH

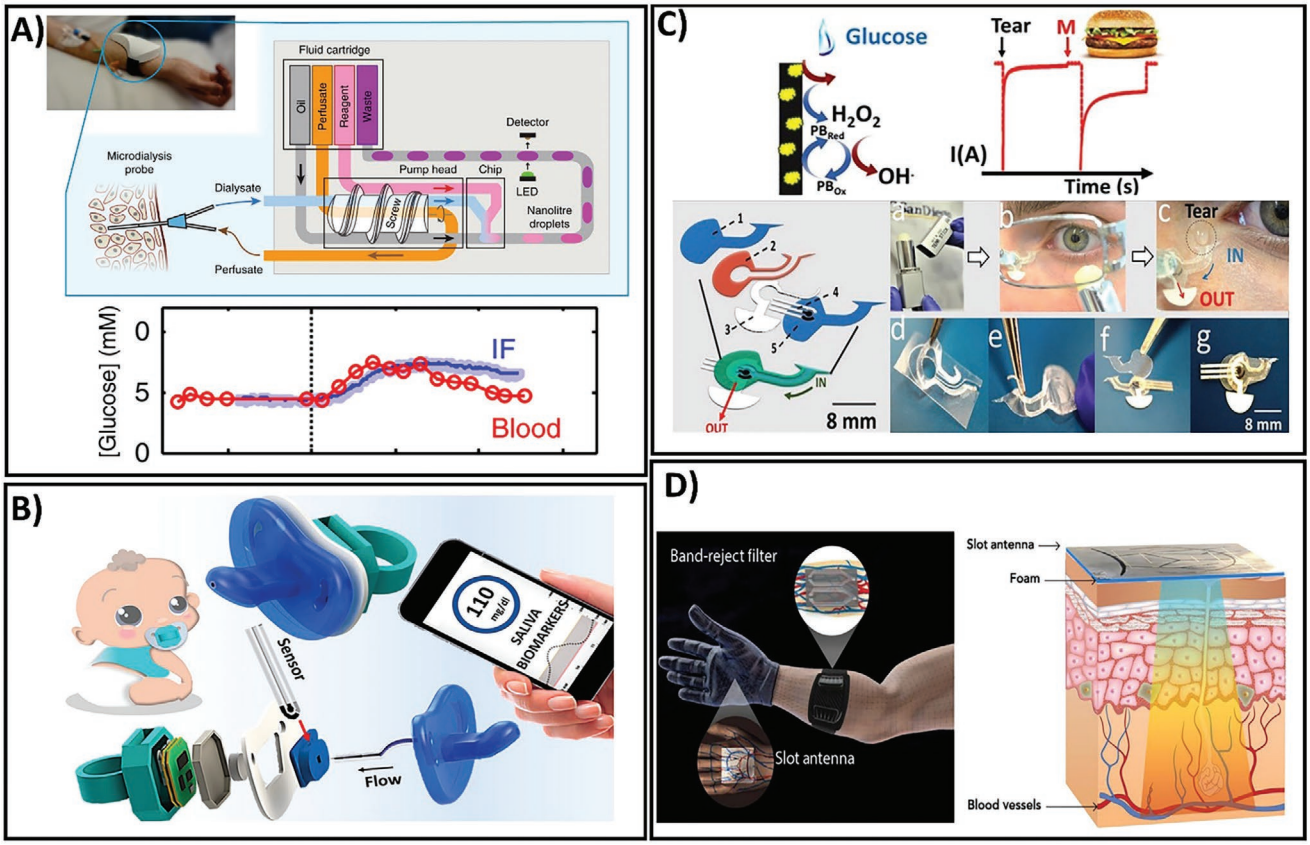

Figure 4. A) Operation and clinical setting for real-time continuous monitoring of ISF glucose concentration using a droplet microfluidic-based sensor. Adapted with permission.[162] Copyright 2019, Springer Nature. B) Enzymatic, electrochemical-based baby-friendly pacifier platform for continuous detection of the saliva glucose levels of infants. Adapted with permission.[170] Copyright 2019 American Chemical Society. C) Process of integration of an eyeglass-based sensing device and on-body tear glucose measurement process. Adapted with permission.[173] Copyright 2019, Elsevier. D) Vasculature anatomy-like sensor for painless, needle-free CGM using blood dielectric properties. Adapted with permission.[166] Copyright 2020, American Association for the Advancement of Science.

3.2. Interstitial Fluid-Based Glucose Monitoring

Although sweat is a desirable biofluid for glucose monitoring, concerns regarding its varied composition, skin contamination, unstable sample volume, uncontrollable sample secretion rate, low glucose concentration, and complexity of sensing device fabrication have driven great interest in wearable sensors for glucose monitoring using interstitial fluid (ISF). Because the molecular components of ISF are similar to those of blood, ISF is a valuable source of molecules with diagnostic potential. Accumulating data have demonstrated a good correlation between glucose levels in the blood and ISF.[191–194] Therefore, ISF is another attractive source of biofluids that provide a large noninvasive source of glucose. However, compared to other body fluids, ISF-based CGM is limited due to the sampling difficulty. Taking advantages of the current technological development, several sensing platforms have been designed for minimally invasive or noninvasive monitoring of glucose levels through ISF.[162–165,167–171] Among the different strategies, micrometer-scale needle patches that allow to access the dermis layer beneath the skin surface in a minimally invasive manner have been widely employed in wearable CGM fabrication for rapid, simple, and continuous monitoring of glucose levels in ISF due to the ease of wearability for users.[164,195,196] Bollella et al. developed a microneedle-based glucose sensor by immobilizing Au-MWCNTs onto the microneedle gold surface and to the methylene blue mediator (MB) to obtain Au-MWCNT/pMB composite.[164] To generate glucose-specific sensing device, Au-MWCNT/pMB composite was functionalized with glucose dehydrogenase. This sensing platform exhibited successful monitoring on healthy volunteers after cycling exercise and after regular meals, making it a potential device for pain-free CGM. Another fully integrated wearable microfluidic sensor has been developed that provides precise and robust means for real-time continuous measurement of glucose levels in ISF.[162] The fabrication procedure is depicted in **Figure 4**A. The sensor was integrated into a small, compact wearable package that comprises a multi-combination of a microfluidic chip, a flow cell, electronics, and a microcontroller connected to an external device via Bluetooth. To measure the glucose level in ISF, a colorimetric assay was implemented due to its rapidness and sensitivity. The as-prepared sensor exhibited a sensitivity of $0.026 \pm 0.002 \times 10^{-3}$ M at a detection limit of 68×10^{-6} M in a linear response up to 8×10^{-3} M after 3 s response time. In vivo validation of the sensing device in healthy human volunteers also showed the expected trends which agree with the results obtained by blood glucose measurement, demonstrating the applicability of the proposed device in real-time physiological

© 2021 Wiley-VCH GmbH

in vivo monitoring. Notably, this sensor did not require human post-setup interaction, providing real-time feedback of glucose levels in the ISF with an accurate detection every 3 s.[162] Despite the challenges facing ISF glucose monitoring, including device operation, sampling procedure, and precise control of extraction rate, ISF-based glucose sensing platforms could provide diverse applications in both research and commercialized-level devices.

3.3. Saliva-Based Glucose Monitoring

Saliva is another important biofluid that has currently attracted attention as a valuable biofluid for noninvasive monitoring and diagnosis due to its abundant availability and continuous supply.[197,198] Saliva is an extracellular fluid that contains a wide array of biomarkers and can be easily obtained in a noninvasive manner either through passive or stimulation methods.[133] Over the past few years, several types of wearable devices for on-body measurement of glucose in saliva have been developed that combine the sampling and sensing steps into a compact, wearable platform.[168–170] In general, the biosensors in the form of a mouthguard or dental accessories contain sensing component integrated with a wireless communication device and a rectifying system that allows the real-time saliva collection in a unidirectional manner. A chemical wearable sensor fully integrated into a pacifier has been developed for glucose monitoring of infants[170] (Figure 4B). The biosensor was fabricated based on glucose oxidase conjugated on a Prussian Blue electrode transducer. The sensor was then integrated with an amperometric circuitry, connected to a Bluetooth system for low-power setup, coupled with an electrochemical detector, and a baby-friendly polymeric nipple for saliva sampling. This design allowed the development of a safe sensing system for a baby's daily life that could address the common difficulties of on-body determination of salivary glucose levels in infants. The device exhibited a successful measurement of glucose levels in artificial saliva with an LOD of 0.04×10^{-3} M in a linear range of 0.1×10^{-3}–1.4×10^{-3} M, which concurred with the glucose concentrations of diabetic saliva. The applicability of the sensor for real-time saliva glucose measurement was demonstrated through the good agreement between the current obtained from the glucose detected in human saliva by the PB-GOx sensor and the commercial blood glucometer signal. Continuous real-time monitoring of saliva glucose was also performed in humans with normal glucose levels and type 1 diabetes. The pacifier sensor showed an apparent change in glucose level before and after a meal in diabetic subjects. Notably, by fully integrating the sensor with wireless transduction, the simplicity of this sensing device was proved in terms of controlling the health of infants and the comfort of the device. Thus, this device is preferable for saliva-based health monitoring of babies. Therefore, this wearable device provides an alternative strategy to address the current issues of blood sampling through invasive access, especially in newborn diseases.

3.4. Tear-Based Glucose Monitoring

Compared to other biofluid-based sensors, the sensing device for tear glucose is relatively less attractive because the glucose levels in tears are often greatly reduced, continuous measurements are often not possible, and the process causes discomfort to the wearers. However, because tear fluid is generally readily available and can be obtained in a noninvasive manner, tear fluid has received exclusive attention as a potential noninvasive body fluid for real-time monitoring of glucose. Several biosensor platforms containing transparent and harmless materials integrated into eyelid or eyeglass have been fabricated for glucose monitoring in tear samples.[172,173] EyeGlass is a common daily accessory that provides convenient access to stimulated tears. An eyeglass nose-bridge pad-based wearable bioelectronic platform was developed for noninvasive monitoring of tear glucose (Figure 4C).[173] The previously developed wearable devices are mostly based on contact lenses, requiring direct contact of the device on eyes, hence causing undesirable irritation. In contrast, this eyeglass nose-bridge sensor contains the electrochemical detector in the nose-bridge, enabling the collection of stimulated tear noninvasively. The biosensor was fabricated by assembling a Prussian blue-mediated carbon electrode into the fluidic device which is then mounted onto the eyeglass nose-bridge pad that enabled stimulated tears to be directly collected over a glucose oxidase-based electrochemical detector. The data obtained by in vitro flow injection analysis showed that the device performed well in terms of detecting tear glucose with a clear, robust linear response, good selectivity in the presence of other metabolites, and highly stable response over a duration of 10 h. Real-time testing of tear glucose levels was performed in healthy human subjects. The eyeglass-based glucose sensor exhibited a rapid response to new stimulated tear samples, which implies success in the detection of changing glucose tear concentrations. The sensor also showed a trend in the measured tear glucose levels, which was well-matched with that of blood glucose values. A 30 min interval during the 2 h experiment was also analyzed, demonstrating its first proof-of-concept for CGM. Another colorful, peacock tail feather-like opal carbon pillar electrode was developed in the form of eyelids for tear glucose sensing.[172] The sensor was prepared by fabricating an opal carbon with bright color and integrating silica crystal templates with high porosity into the sensor, thus enabling sensitive detection while ensuring high energy storage. The sensing device showed good performance with a detection limit of 12×10^{-6} M and good correspondence between tear glucose levels and blood glucose concentration when using tear samples from three volunteers during eye movement. From a clinical viewpoint, the adaptation of this wearable sensing platform to physiological monitoring of diseases as well as daily healthcare could provide an ideal solution for healthcare and beauty at the same time.

3.5. Noninvasive Blood-Based Glucose Monitoring

In addition to the conventional optical and electrochemical sensors, during the last several years, electromagnetism (EM) has emerged as a promising technology for noninvasive CGM.[199,200] In principle, glucose monitoring by EM is based on the specific dielectric properties of blood altered by glucose concentration. The presence and fluctuation of blood glucose

© 2021 Wiley-VCH GmbH

Table 4. Comparative analysis of glucose sensing performance in various body fluids toward wearable CGM.

Properties	Blood	Urine	Sweat	Saliva	ISF	Tear
Glucose concentration	✓✓✓	✓✓	✓	✓	✓✓	✓
Correlation to blood glucose level	✓✓✓	✓✓	✓	✓	✓✓	✓
Reliability	✓✓✓	✓✓	✓	✓	✓✓	✓
Invasiveness	✓✓✓	–	–	–	✓✓	✓
Sampling difficulty	✓✓✓	✓	✓	✓	✓✓	✓✓
Comfort	–	✓	✓	–	–	–
Pain or irritation during sampling	✓✓✓	–	–	–	✓	✓
Safety	–	✓	✓	–	–	–
Real-time, continuous measuring ability	–	–	✓	–	✓	✓
Variation between sampling site	–	–	✓	–	✓	–
Sample homogeneity	✓	✓	–	–	✓	✓
Controlling ability of secretion rate	✓	✓	–	–	✓	–
Sample reproduction	✓	–	–	✓	✓	–
Requirement of stimulation or activity	–	–	✓	✓	–	✓
Portability	✓	✓	✓	✓	✓	✓
Point-of-care suitability	✓	✓	✓	✓	✓	✓
Accuracy	✓✓✓	✓✓✓	✓	✓	✓✓	✓
Interference	✓	✓	✓	✓	✓	✓
Dependence of lifestyle, activity, diet,...	–	–	✓	✓	–	✓
Wearable comfort	–	–	✓✓✓	✓✓	✓✓	✓
Instrument cost-effectiveness	✓	✓	–	–	–	–

Level of property: (✓) low, (✓✓) moderate, (✓✓✓) high.

levels lead to variations in the dielectric constant of blood, which can be recorded by EM waves and converted into glucose concentration values. This method allows the direct measurement of blood glucose levels noninvasively, which helps address the drawbacks of other wearable sensor types, including time delay or sensitivity. Recently, a first-of-its-kind, noninvasive, direct glucose-monitoring sensor from blood was developed, which holds promise for the development of "closed-loop" therapy (Figure 4D).[166] For sensor fabrication, two different electromagnetism-based parts were integrated into a single system, including a multiband-reject filter and a multiband slot antenna printed on a flexible polyethylene terephthalate using silver nano-ink. Several modifications have been introduced to achieve high accuracy in terms of glucose variations. These include the simulation of the vascular anatomies into the sensor structure that ensures improved accuracy and sensitivity of glucose level estimation. Most significantly, the proposed antenna was designed for on-body matching when integrated onto a human hand model that provides good contact between the antenna and the human body. Consequently, highly sensitive analysis of the variations blood glucose levels with no delay was achieved, demonstrating the efficacy of direct monitoring of glucose from the blood. This sensor presented a high sensitivity toward glucose variations compared to other interferent compositions. The sensor was also validated for its applicability in the detection of real-time glucose levels. Notably, by combining the antenna and the filter in a single platform, this sensing device could measure glucose levels accurately regardless of the individual's characteristics, which is a great challenge for current glucose sensors in human trials.[201]

Overall, the adoption of alternative biofluids and blood dielectric properties for noninvasive tracking of glucose levels by advanced nanomaterial-based wearable devices showed immense opportunity to improve glycemic control and public healthcare. Regarding on-body glucose monitoring, each body fluid presents its advantages and drawbacks, as summarized in **Table 4**, making it a significant factor in establishing a standardized detection approach for noninvasive glucose monitoring. However, with the latest developments in the integration of nanomaterial-based sensors into wearable accessories, such "touch and sense" platforms will provide a useful tool for real-time monitoring of glucose levels in a noninvasive fashion. This comparative information could increase the further interest of researchers as well as clinical practicians to exploit the superior remote CGM devices for better control of diabetes with the most accurate and reliable glucose measurement without direct communication to patients during the on-going COVID-19 pandemic and in the future.

4. Conclusions, Challenges, and Prospects

The number of patients with diabetes is rapidly growing worldwide, and diabetes has become one of the world's fastest-growing chronic conditions. Because the burden of diabetes is enormous due to its high prevalence and increasing risks

© 2021 Wiley-VCH GmbH

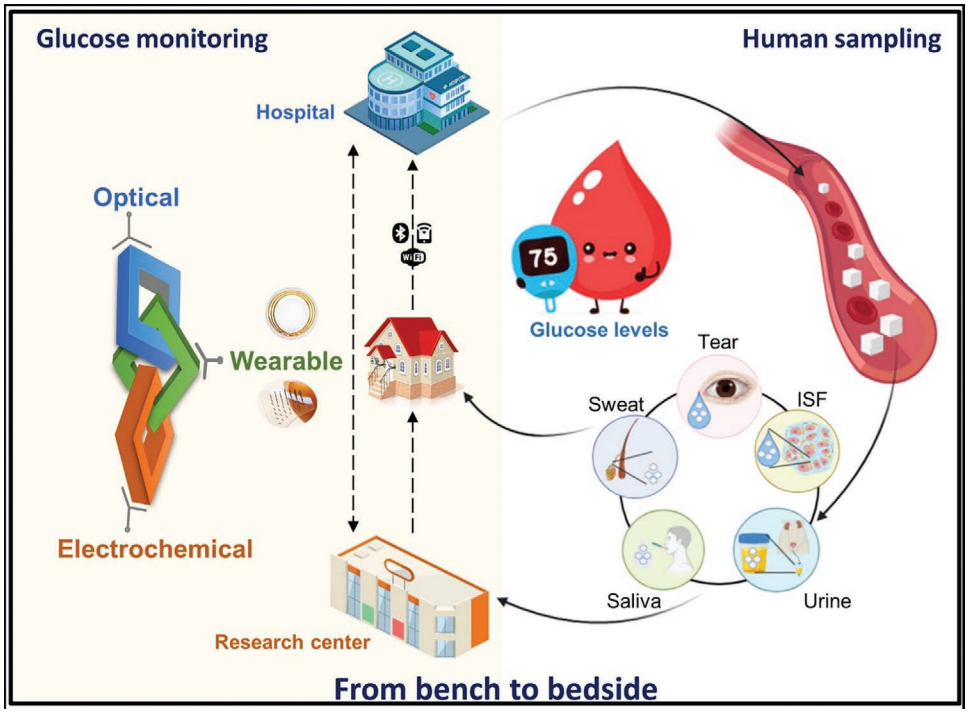

Figure 5. Conceptual illustration of the development process from hospital invasive detection to in-house noninvasive monitoring of glucose levels in biofluids using wearable sensors for collaborative applications in healthcare and research.

of cardiovascular and other diseases, it is essential to improve the methods of prevention and management of diabetes to reduce growing global problems. Importantly, the pandemic spread of the COVID-19 is increasing daily, with millions of deaths reported worldwide, boosting the requirement for glucose self-monitoring, which is important for the efficient management of diabetes and the COVID-19 pandemic. This has attracted researchers' attention to explore an accurate and reliable glucose-monitoring device for not only better controlling of diabetes during this pandemic but also contributing to avoid the spread of coronavirus. This review details the current trends during the COVID-19 pandemic period (2019–2020) in terms of glucose measurement using different techniques for real-time, noninvasive glucose monitoring. Studies on glucose monitoring during the last 2 years based on optical and electrochemical approaches with/without the use of enzymes were reviewed, and their advantages and limitations were discussed. More importantly, current wearable devices for noninvasive CGM have been presented to highlight the state-of-art wearable, flexible sensors with the integration of diverse signal transmission methods that allow remote data assessment and glucose level control by CGM (**Figure 5**), joining global effort to end COVID-19 pandemic.

Nanomaterials have provided advantages in terms of enhancing the benefits of sensor platforms because of the increase in surface area to volume ratios and straightforward surface functionalization such as miniaturization; in addition, they have various advantages such as good portability, high sensitivity, large linear range, and rapid signal response times. Both optical and electrochemical sensors for glucose have benefited from smart nanomaterials with high sensitivity and specificity. Electrochemical sensors incorporating GOx enzymes with nanomaterials improve the sensitivity and time response by taking advantage of the high surface area and more efficient electron transfer from the enzyme to the electrode. Although the GOx enzymes can increase the selectivity of the glucose sensor, the intrinsically poorer stability of the enzyme as a biological molecule is a drawback for the sensors, which affects the storage lifetime of glucose sensors. To address the limitation of short-term storage, direct oxidation glucose sensors have been developed based on nanomaterials in that focus on exploiting different materials and fabrication processes. However, the weaknesses of recent nanomaterial-based glucose sensors are their poor biocompatibility, time-consuming preparation process, and requirements for complicated equipment. Importantly, because of the difficulty of CGM using these sensors, significant variabilities of glucose levels that are reflective of a patient's physiological state are often ignored, especially in hypoglycemia, which is common in insulin-treated patients with diabetes and more dangerous than hyperglycemia. Furthermore, invasive monitoring leads to discomfort and pain for patients with diabetes and exposes patients to risks of infections, resulting in poor results of daily measurements. These glucose-monitoring techniques should be applied in hospitals with more experienced technicians for evaluating diabetes status. Thus, the challenge of exploring patient-friendly glucose sensing devices with high selectivity and sensitivity that can be readily applied for personalized, continuous glucose measurement still exists.

Several studies have proven the benefits of applying alternative biofluids such as saliva, tears, and sweat as feasible analytes for glucose monitoring; such methods would reduce pain and

 © 2021 Wiley-VCH GmbH

may be convenient and patient-friendly. In the current decade, extensive efforts have been made to shift the glucose sensing system toward in-house monitoring and remote management of patients with diabetes. The adoption of nanomaterials and economical fabrication techniques has led to significant improvements in wearable glucose sensors for other biofluids, including highly sensitive, noninvasive, and painless protocols and continuous real-time monitoring, which can provide the patient with self-monitoring solutions. The glucose levels measured by some wearable glucose sensors have been confirmed to highly agree with blood glucose levels; such sensors can be utilized as body-compliant wearable platforms. Until now, several home-trial devices have been approved; unfortunately, no long-term use of these products has been reported. However, there are considerable challenges regarding the establishment of standard sets, tools, and guidelines for accurate assessment and monitoring. Although other biofluids act as useful noninvasive analytes for glucose monitoring, the achievement of reliable correlations between blood glucose and the glucose levels of other biofluids still poses a challenge. The interference from other glucose sources or biomaterials in biofluids could affect the performance of wearable glucose sensors. Selective fresh glucose uptake from biofluids is important for the development of reliable wearable monitoring platforms. The next generation of wearable glucose systems should focus on accurate glucose measurement with other physiological parameters such as pH, temperature, or humidity to improve accuracy by enhancing the correlation with blood glucose levels. Furthermore, a more reliable parameter against physiological variance among individuals should be verified to authenticate the validity and reliability of wearable sensors compared with blood glucose sensors. In addition to individual devices that are pending for further research, biofluid specimen sampling protocols, emerging materials, and favorable device designs should be improved to encourage patient friendliness. Additionally, alternatives for energy generation methods should be considered to ensure a fully implanted and easy-to-wear device, especially for electrochemical glucose sensor systems. Finally, wearable glucose monitoring devices that are cost-effective and patient-friendly and have an appropriate response to changing blood glucose levels, high correlation with blood glucose levels, long-term stability, consistency between individuals, and continuous reliability should be explored to overcome the current challenges of wearable glucose-monitoring systems. After consideration of these scientific problems, the feasibility of wearable glucose monitoring devices must be successfully validated through qualifying clinical trials for the approval of these devices for commercial and medical applications with guaranteed personal data security. Henceforth, through technological advances, wearable glucose monitoring platforms that have comparable reliability to blood glucose systems and exhibit a promising diagnostic potential in satisfying both patient-friendly paradigms and public health can be developed. Through telehealth, these wearable devices represent a critical alternative form of health care, shifting from traditional face-to-face clinical consultations to remote intervention. The feasibility of on-body CGM plays an important role in limiting health-care worker exposures to COVID-19. To successfully place the technology in diabetes management during and after COVID-19 pandemic, the standardized protocols from patients and residents to health-care workers should be finalized to provide diabetes comprehensive care without increasing the risk from coronavirus. Taking advantage of CGM technology not only contributes to efficiently prevent the spread of COVID-19 during this pandemic but also paves the way for the personalized diabetes medicine in the future. With state-of-art innovation of wearable gadgets, we will witness the emergence of a new revolution for CGM and diabetes diagnosis from research to market, making effective diabetic healthcare programs rely entirely on wearable glucose monitoring, leading the way to the brighter future of diabetes management.

Acknowledgements

L.M.T.P. and T.A.T.V. contributed equally to this work. This research was supported by the National Research Foundation of Korea (NRF-2020M3A9E410438511, NRF-2019R1A2C1088680) and by the GRRC program of Gyeonggi province (GRRC-Gachon2020(B01), AI-based Medical Image Analysis).

Conflict of Interest

The authors declare no conflict of interest.

Keywords

COVID-19, electrochemical sensors, glucose monitoring, nanomaterials, noninvasive sensors, wearable CGM

Received: January 5, 2021
Revised: February 18, 2021
Published online: May 6, 2021

[1] D. Baud, X. Qi, K. Nielsen-Saines, D. Musso, L. Pomar, G. Favre, *Lancet Infect. Dis.* **2020**, *20*, 773.
[2] W. Guo, M. Li, Y. Dong, H. Zhou, Z. Zhang, C. Tian, R. Qin, H. Wang, Y. Shen, K. Du, L. Zhao, H. Fan, S. Luo, D. Hu, *Diabetes/Metab. Res. Rev.* **2020**, *36*, e3319.
[3] J. A. Critchley, I. M. Carey, T. Harris, S. DeWilde, F. J. Hosking, D. G. Cook, *Diabetes Care* **2018**, *41*, 2127.
[4] G. Shehav-Zaltzman, G. Segal, N. Konvalina, A. Tirosh, *Diabetes Care* **2020**, *43*, e75.
[5] D. S. Keeble, M. Z. Farland, J. Eaddy, *Am. Fam. Physician* **2014**, *90*, 524.
[6] L. Monnier, C. Colette, *Diabetes Care* **2008**, *31*, S150.
[7] A. Deeb, M. Ziaullah, M. Akle, K. Strauss, *J. Diabetes Sci. Technol.* **2019**, *13*, 146.
[8] K. Tian, M. Prestgard, A. Tiwari, *Mater. Sci. Eng., C* **2014**, *41*, 100.
[9] I. L. Jernelv, K. Milenko, S. S. Fuglerud, D. R. Hjelme, R. Ellingsen, A. Aksnes, *Appl. Spectrosc. Rev.* **2019**, *54*, 543.
[10] H. Teymourian, A. Barfidokht, J. Wang, *Chem. Soc. Rev.* **2020**, *49*, 7671.
[11] P. Damborský, J. Švitel, J. Katrlík, *Essays Biochem.* **2016**, *60*, 91.
[12] C. Chen, J. Wang, *Analyst* **2020**, *145*, 1605.
[13] S. Rashtbari, G. Dehghan, M. Amini, *Anal. Chim. Acta* **2020**, *1110*, 98.
[14] E. T. Bushman, V. C. Jauk, J. M. Szychowski, S. Mazzoni, A. T. Tita, L. M. Harper, *Am. J. Obstet. Gynecol.* **2020**, *222*, S161.
[15] K. Neubauerova, M. C. C. G. Carneiro, L. R. Rodrigues, F. T. C. Moreira, M. G. F. Sales, *Sens. Bio-Sens. Res.* **2020**, *29*, 100368.

 © 2021 Wiley-VCH GmbH

[16] Q. Lu, T. Huang, J. Zhou, Y. Zeng, C. Wu, M. Liu, H. Li, Y. Zhang, S. Yao, *Spectrochim. Acta, Part A* **2021**, *244*, 118893.
[17] P. Hu, R. Zhou, D. Wang, H. Luo, X. Xiong, K. Huang, L. Li, P. Chen, *Sens. Actuators, B* **2020**, *308*, 127702.
[18] X. T. Zheng, Y. Choi, D. G. G. Phua, Y. N. Tan, *Bioconjugate Chem.* **2020**, *31*, 754.
[19] G.-L. Hong, H.-H. Deng, H.-L. Zhao, Z.-Y. Zou, K.-Y. Huang, H.-P. Peng, Y.-H. Liu, W. Chen, *J. Pharm. Biomed. Anal.* **2020**, *189*, 113480.
[20] J. Lu, H. Zhang, S. Li, S. Guo, L. Shen, T. Zhou, H. Zhong, L. Wu, Q. Meng, Y. Zhang, *Inorg. Chem.* **2020**, *59*, 3152.
[21] G. Zeng, M. Duan, Y. Xu, F. Ge, W. Wang, *Spectrochim. Acta, Part A* **2020**, *241*, 118649.
[22] Y. Kang, X. Xue, W. Wang, Y. Fan, W. Li, T. Ma, F. Zhao, Z. Zhang, *J. Phys. Chem. C* **2020**, *124*, 21054.
[23] Y. Cui, X. Lai, K. Liu, B. Liang, G. Ma, L. Wang, *RSC Adv.* **2020**, *10*, 7012.
[24] J. Li, X. Li, R. Weng, T. Qiang, X. Wang, *Sens. Actuators, B* **2020**, *304*, 127349.
[25] Z. Long, Y. Liang, L. Feng, H. Zhang, M. Liu, T. Xu, *Nanoscale* **2020**, *12*, 10809.
[26] T. T. Wang, K. Guo, X. M. Hu, J. Liang, X. D. Li, Z. F. Zhang, J. Xie, *Chemosensors* **2020**, *8*, 10.
[27] C. B. Ma, Y. Zhang, Q. Liu, Y. Du, E. Wang, *Anal. Chem.* **2020**, *92*, 5319.
[28] P. Du, Q. Niu, J. Chen, Y. Chen, J. Zhao, X. Lu, *Anal. Chem.* **2020**, *92*, 7980.
[29] G. Pandey, R. Chaudhari, B. Joshi, S. Choudhary, J. Kaur, A. Joshi, *Sci. Rep.* **2019**, *9*, 5029.
[30] Z. Zhao, Y. Huang, W. Liu, F. Ye, S. Zhao, *ACS Sustainable Chem. Eng.* **2020**, *8*, 4481.
[31] I. Brice, K. Grundsteins, A. Atvars, J. Alnis, R. Viter, A. Ramanavicius, *Sens. Actuators, B* **2020**, *318*, 128004.
[32] T. H. Fereja, S. A. Kitte, M. N. Zafar, M. I. Halawa, S. Han, W. Zhang, G. Xu, *Analyst* **2020**, *145*, 1041.
[33] Q. Liu, F. Aouidat, P. Sacco, E. Marsich, N. Djaker, J. Spadavecchia, *Colloids Surf., B* **2020**, *185*, 110588.
[34] P. Sengupta, K. Pramanik, P. Datta, P. Sarkar, *Biosens. Bioelectron.* **2020**, *154*, 112072.
[35] J. Zhang, X. Dai, Z.-L. Song, R. Han, L. Ma, G.-C. Fan, X. Luo, *Sens. Actuators, B* **2020**, *304*, 127304.
[36] H. Pezhhan, M. Akhond, M. Shamsipur, *J. Lumin.* **2020**, *228*, 117604.
[37] H. Medetalibeyoglu, G. Kotan, N. Atar, M. L. Yola, *Anal. Chim. Acta* **2020**, *1139*, 100.
[38] X. Niu, X. Li, J. Pan, Y. He, F. Qiu, Y. Yan, *RSC Adv.* **2016**, *6*, 84893.
[39] E. Sehit, Z. Altintas, *Biosens. Bioelectron.* **2020**, *159*, 112165.
[40] D. Grieshaber, R. MacKenzie, J. Vörös, E. Reimhult, *Sensors* **2008**, *8*, 1400.
[41] Z. Khosroshahi, F. Karimzadeh, M. Kharaziha, A. Allafchian, *Mater. Sci. Eng., C* **2020**, *108*, 110216.
[42] P. N. Asrami, P. A. Azar, M. S. Tehrani, S. A. Mozaffari, *Front. Chem.* **2020**, *8*, 503.
[43] A. Górska, B. Paczosa-Bator, J. Wyrwa, R. Piech, *Electroanalysis* **2020**, *32*, 1875.
[44] H. Zhang, T. Fan, W. Chen, Y. Li, B. Wang, *Bioact. Mater.* **2020**, *5*, 1071.
[45] Y. X. Wen, S. G. Liu, B. X. Tao, H. Q. Luo, N. B. Li, *Sens. Actuators, B* **2020**, *304*, 127279.
[46] J. Chen, X. Zheng, Y. Li, H. Zheng, Y. Liu, S.-I. Suye, *J. Electrochem. Soc.* **2020**, *167*, 067502.
[47] J. Chen, X. Zheng, Y. Li, H. Zheng, Y. Liu, S. I. Suye, *Sensors* **2020**, *20*, 3365.
[48] L. D. Nguyen, T. M. Huynh, T. S. V. Nguyen, D. N. Le, R. Baptist, T. C. D. Doan, C. M. Dang, *J. Electroanal. Chem.* **2020**, *873*, 114396.
[49] H. Zheng, M. Liu, Z. Yan, J. Chen, *Microchem. J.* **2020**, *152*, 104266.
[50] X. Xiao, Y. Wang, H. Cheng, Y. Cui, Y. Xu, T. Yang, D. Zhang, X. Xu, *Mater. Chem. Phys.* **2020**, *240*, 122202.
[51] M. Usman, L. Pan, A. Farid, A. S. Khan, Z. Yongpeng, M. A. Khan, M. Hashim, *Carbon* **2020**, *858*, 113810.
[52] L. Wang, X. Miao, Y. Qu, C. Duan, B. Wang, Q. Yu, J. Gao, D. Song, Y. Li, Z. Yin, *J. Electroanal. Chem.* **2020**, *858*, 113810.
[53] X. Gao, X. Du, D. Liu, H. Gao, P. Wang, J. Yang, *Sci. Rep.* **2020**, *10*, 1365.
[54] M. Ma, Y. Zhou, J. Li, Z. Ge, H. He, T. Tao, Z. Cai, X. Wang, G. Chang, Y. He, *Analyst* **2020**, *145*, 887.
[55] N. Khalaf, T. Ahamad, M. Naushad, N. Al-Hokbany, S. I. Al-Saeedi, S. Almotairi, S. M. Alshehri, *Int. J. Biol. Macromol.* **2020**, *146*, 763.
[56] E. Muthusankar, S. M. Wabaidur, Z. A. Alothman, M. R. Johan, V. K. Ponnusamy, D. Ragupathy, *Ionics* **2020**, *26*, 6341.
[57] A. K. Manna, P. Guha, V. J. Solanki, S. Srivastava, S. Varma, *J. Solid State Electrochem.* **2020**, *24*, 1647.
[58] S. Mojtahedi, M. Karimipour, E. Heydari-Bafrooei, M. Molaei, *Microchem. J.* **2020**, *159*, 105405.
[59] M. Waqas, L. Wu, H. Tang, C. Liu, Y. Fan, Z. Jiang, X. Wang, J. Zhong, W. Chen, *ACS Appl. Nano Mater.* **2020**, *3*, 4788.
[60] R. Ahmad, M. Khan, M. R. Khan, N. Tripathy, M. I. R. Khan, P. Mishra, M. A. Syed, A. Khosla, *Microsyst. Technol.* **2020**, 1.
[61] M. Kang, H. Zhou, N. Zhao, *CrystEngComm* **2020**, *22*, 35.
[62] B. Yang, N. Han, L. Zhang, S. Yi, Z. Zhang, Y. Wang, Y. Zhou, D. Chen, Y. Gao, *Appl. Surf. Sci.* **2020**, *534*, 147596.
[63] M. Ezzati, S. Shahrokhian, H. Hosseini, *ACS Sustainable Chem. Eng.* **2020**, *8*, 14340.
[64] D. Chu, F. Li, X. Song, H. Ma, L. Tan, H. Pang, X. Wang, D. Guo, B. Xiao, *J. Colloid Interface Sci.* **2020**, *568*, 130.
[65] L. Lin, S. Weng, Y. Zheng, X. Liu, S. Ying, F. Chen, D. You, *J. Electroanal. Chem.* **2020**, *865*, 114147.
[66] H. Karimi-Maleh, K. Cellat, K. Arıkan, A. Savk, F. Karimi, F. Şen, *Mater. Chem. Phys.* **2020**, *250*, 123042.
[67] L. Tang, K. Huan, D. Deng, L. Han, Z. Zeng, L. Luo, *Colloids Surf., B* **2020**, *188*, 110797.
[68] F. Zhou, C. You, Q. Wang, Y. Chen, Z. Wang, Z. Zeng, X. Sun, K. Huang, X. Xiong, *J. Electroanal. Chem.* **2020**, *876*, 114477.
[69] C. Wei, X. Zou, Q. Liu, S. Li, C. Kang, W. Xiang, *Electrochim. Acta* **2020**, *334*, 135630.
[70] N. Singer, R. G. Pillai, A. I. Johnson, K. D. Harris, A. B. Jemere, *Microchim. Acta* **2020**, *187*, 196.
[71] J. Zhang, Y. Sun, X. Li, J. Xu, *Sci. Rep.* **2019**, *9*, 18121.
[72] B.-R. Huang, D. Kathiravan, C.-W. Wu, W.-L. Yang, *ACS Appl. Bio Mater.* **2020**, *3*, 5966.
[73] S. Wu, Y. Zhang, L. Liu, W. Fan, *Mater. Lett.* **2020**, *276*, 128253.
[74] S. Liu, J. Zhao, L. Qin, G. Liu, Q. Zhang, J. Li, *J. Mater. Sci.* **2020**, *55*, 337.
[75] Z. Wu, J. Zhao, Z. Yin, X. Wang, Z. Li, X. Wang, *Sens. Actuators, B* **2020**, *312*, 127978.
[76] X. H. Shi, K. J. Xu, *Mater. Sci. Semicond. Process.* **2017**, *58*, 1.
[77] L. He, Q. Zhang, C. Gong, H. Liu, F. Hu, F. Zhong, G. Wang, H. Su, S. Wen, S. Xiang, B. Zhang, *Sens. Actuators, B* **2020**, *310*, 127842.
[78] Y.-Y. Li, P. Kang, H.-Q. Huang, Z.-G. Liu, G. Li, Z. Guo, X.-J. Huang, *Sens. Actuators, B* **2020**, *307*, 127639.
[79] L. Lamiri, O. Belgherbi, C. Dehchar, S. Laidoudi, A. Tounsi, B. Nessark, F. Habelhames, A. Hamam, B. Gourari, *Synth. Met.* **2020**, *266*, 116437.
[80] A. Salah, N. Al-Ansi, S. Adlat, M. Bawa, Y. He, X. Bo, L. Guo, *J. Alloys Compd.* **2019**, *792*, 50.
[81] Y. P. Palve, N. Jha, *Mater. Chem. Phys.* **2020**, *240*, 122086.
[82] Z. Xue, L. Jia, R.-R. Zhu, L. Du, Q.-H. Zhao, *J. Electroanal. Chem.* **2020**, *858*, 113783.

 © 2021 Wiley-VCH GmbH

[83] H. Yin, T. Zhan, J. Chen, L. Wang, J. Gong, S. Zhao, Z. Ji, *J. Mater. Sci.: Mater. Electron.* **2020**, *31*, 4323.
[84] Q. Zhu, S. Hu, L. Zhang, Y. Li, C. Carraro, R. Maboudian, W. Wei, A. Liu, Y. Zhang, S. Liu, *Sens. Actuators, B* **2020**, *313*, 128031.
[85] J. Liu, H. Zhang, X. Xiaochuan, A. ul Ahmad, D. Xue, H. Huang, N. Xu, Q. Xi, W. Guo, H. Liang, *Sens. Actuators, A* **2020**, *312*, 112128.
[86] S. H. Baek, J. Roh, C. Y. Park, M. W. Kim, R. Shi, S. K. Kailasa, T. J. Park, *Mater. Sci. Eng., C* **2020**, *107*, 110273.
[87] J. Xu, K. Xu, Y. Han, D. Wang, X. Li, T. Hu, H. Yi, Z. Ni, *Analyst* **2020**, *145*, 5141.
[88] H. Yoon, J. Nah, H. Kim, S. Ko, M. Sharifuzzaman, S. C. Barman, X. Xuan, J. Kim, J. Y. Park, *Sens. Actuators, B* **2020**, *311*, 127866.
[89] K. Sakdaphetsiri, T. Thaweeskulchai, A. Schulte, *Chem. Commun.* **2020**, *56*, 7132.
[90] E. Sehit, J. Drzazgowska, D. Buchenau, C. Yesildag, M. Lensen, Z. Altintas, *Biosens. Bioelectron.* **2020**, *165*, 112432.
[91] M. Eryiğit, E. Çepni, B. Kurt Urhan, H. Öztürk Doğan, T. Öznülüer Özer, *Synth. Met.* **2020**, *268*, 116488.
[92] S. Sun, N. Shi, X. Liao, B. Zhang, G. Yin, Z. Huang, X. Chen, X. Pu, *Appl. Surf. Sci.* **2020**, *529*, 147067.
[93] D. He, M. Wang, X. Wang, S. Feng, J. Chen, P. Jiang, *J. Solid State Chem.* **2020**, *284*, 121214.
[94] Z. Wang, J. Zhang, R. Jian, J. Liao, X. Xiong, K. Huang, *Microchem. J.* **2020**, *159*, 105396.
[95] L. Jayasingha, C. Jayathilaka, R. Kumara, K. Ohara, M. Kaumal, S. Gunewardene, D. Dissanayake, S. Jayanetti, *Electrochim. Acta* **2020**, *329*, 135177.
[96] S. D. Rani, R. Ramachandran, S. Sheet, M. A. Aziz, Y. S. Lee, A. G. Al-Sehemi, M. Pannipara, Y. Xia, S.-Y. Tsai, F.-L. Ng, *Sens. Actuators, B* **2020**, *312*, 127886.
[97] A. K. Mishra, D. K. Jarwal, B. Mukherjee, A. Kumar, S. Ratan, M. R. Tripathy, *Sci. Rep.* **2020**, *10*, 11451.
[98] E. Rafatmah, B. Hemmateenejad, *Sens. Actuators, B* **2020**, *304*, 127335.
[99] S. Khan, M. A. Rasheed, A. Waheed, A. Shah, A. Mahmood, T. Ali, A. Nisar, M. Ahmad, S. Karim, G. Ali, *Mater. Sci. Semicond. Process.* **2020**, *109*, 104953.
[100] P. J. Lynch, A. A. Graf, S. P. Ogilvie, M. J. Large, J. P. Salvage, A. B. Dalton, *J. Mater. Chem. B* **2020**, *8*, 7733.
[101] Q. Guo, T. Wu, L. Liu, Y. He, D. Liu, T. You, *J. Alloys Compd.* **2020**, *819*, 153376.
[102] A. R. Abbasi, M. Yousefshahi, K. Daasbjerg, *J. Inorg. Organomet. Polym.* **2020**, *30*, 2027.
[103] T. Meng, H. Jia, H. Ye, T. Zeng, X. Yang, H. Wang, Y. Zhang, *J. Colloid Interface Sci.* **2020**, *560*, 1.
[104] J. Ye, D. Deng, Y. Wang, L. Luo, K. Qian, S. Cao, X. Feng, *Sens. Actuators, B* **2020**, *305*, 127473.
[105] F. Wang, X. Ding, X. Niu, X. Liu, W. Wang, J. Zhang, *Carbohydr. Polym.* **2020**, *247*, 116647.
[106] Y. Luo, Q. Wang, J. Li, F. Xu, L. Sun, Y. Bu, Y. Zou, H.-B. Kraatz, F. Rosei, *Inorg. Chem. Front.* **2020**, *7*, 1512.
[107] K. Kim, S. Kim, H. N. Lee, Y. M. Park, Y.-S. Bae, H.-J. Kim, *Appl. Surf. Sci.* **2019**, *479*, 720.
[108] Z. Haghparas, Z. Kordrostami, M. Sorouri, M. Rajabzadeh, R. Khalifeh, *Biotechnol. Bioprocess Eng.* **2020**, *25*, 528.
[109] Y. Zhang, Y.-Q. Liu, Y. Bai, W. Chu, J. Sh, *Sens. Actuators, B* **2020**, *309*, 127779.
[110] J. Qian, Y. Wang, J. Pan, Z. Chen, C. Wang, J. Chen, Z. Wu, Yangyue, *Mater. Chem. Phys.* **2020**, *239*, 122051.
[111] R. G. Rocha, R. M. Cardoso, P. J. Zambiazi, S. V. F. Castro, T. V. B. Ferraz, G. D. O. Aparecido, J. A. Bonacin, R. A. A. Munoz, E. M. Richter, *Anal. Chim. Acta* **2020**, *1132*, 1.
[112] A. Inyang, G. Kibambo, M. Palmer, F. Cummings, M. Masikini, C. Sunday, M. Chowdhury, *Thin Solid Films* **2020**, *709*, 138244.
[113] L. He, Q. Zhang, C. Gong, H. Liu, F. Hu, F. Zhong, G. Wang, H. Su, S. Wen, S. Xiang, *Sens. Actuators, B* **2020**, *310*, 127842.
[114] L. Wang, W. Lu, W. Zhu, H. Wu, F. Wang, X. Xu, *Sens. Actuators, B* **2020**, *304*, 127330.
[115] H. Li, C. Guo, C. Liu, L. Ge, F. Li, *Analyst* **2020**, *145*, 4041.
[116] B. Kurt Urhan, Ü. Demir, T. Öznülüer Özer, H. Öztürk Doğan, *Thin Solid Films* **2020**, *693*, 137695.
[117] X. Xu, C. Liu, W. Zhang, X. Zou, *Sens. Actuators, B* **2020**, *324*, 128720.
[118] H. Xu, F. Han, C. Xia, S. Wang, S. Zhuiykov, G. Zheng, *Electrochim. Acta* **2020**, *331*, 135295.
[119] S. Bag, A. Baksi, S. H. Nandam, D. Wang, X. Ye, J. Ghosh, T. Pradeep, H. Hahn, *ACS Nano* **2020**, *14*, 5543.
[120] S. Guo, C. Zhang, M. Yang, Y. Zhou, C. Bi, Q. Lv, N. Ma, *Anal. Chim. Acta* **2020**, *1109*, 130.
[121] P. Chakraborty, S. Dhar, N. Deka, K. Debnath, S. P. Mondal, *Sens. Actuators, B* **2020**, *302*, 127134.
[122] Q. Zhang, F. Zhang, L. Yu, Q. Kang, Y. Chen, D. Shen, *Microchim. Acta* **2020**, *187*, 244.
[123] J. Wang, Y. Liu, L. Cheng, R. Chen, H. Ni, *J. Alloys Compd.* **2020**, *821*, 153510.
[124] Y. Zhang, N. Li, Y. Xiang, D. Wang, P. Zhang, Y. Wang, S. Lu, R. Xu, J. Zhao, *Carbon* **2020**, *156*, 506.
[125] C. Huang, Y. Wang, X. Li, L. Ren, J. Zhao, Y. Hu, L. Zhang, G. Fan, J. Xu, X. Gu, Z. Cheng, T. Yu, J. Xia, Y. Wei, W. Wu, X. Xie, W. Yin, H. Li, M. Liu, Y. Xiao, H. Gao, L. Guo, J. Xie, G. Wang, R. Jiang, Z. Gao, Q. Jin, J. Wang, B. Cao, *Lancet* **2020**, *395*, 497.
[126] E. Ushigome, M. Yamazaki, M. Hamaguchi, T. Ito, S. Matsubara, Y. Tsuchido, Y. Kasamatsu, M. Nakanishi, N. Fujita, M. Fukui, *Diabetes Technol. Ther.* **2021**, *23*, 78.
[127] S. Reutrakul, M. Genco, H. Salinas, R. M. Sargis, C. Paul, Y. Eisenberg, J. Fang, R. N. Caskey, S. Henkle, S. Fatoorehchi, A. Osta, P. Srivastava, A. Johnson, S. E. Messmer, M. Barnes, S. Pratuangtham, B. T. Layden, *Diabetes Care* **2020**, *43*, e137.
[128] R. J. Galindo, G. Aleppo, D. C. Klonoff, E. K. Spanakis, S. Agarwal, P. Vellanki, D. E. Olson, G. E. Umpierrez, G. M. Davis, F. J. Pasquel, *J. Diabetes Sci. Technol.* **2020**, *14*, 822.
[129] F. Zhou, T. Yu, R. Du, G. Fan, Y. Liu, Z. Liu, J. Xiang, Y. Wang, B. Song, X. Gu, L. Guan, Y. Wei, H. Li, X. Wu, J. Xu, S. Tu, Y. Zhang, H. Chen, B. Cao, *Lancet* **2020**, *395*, 1054.
[130] S. Lim, J. H. Bae, H.-S. Kwon, M. A. Nauck, *Nat. Rev. Endocrinol.* **2020**, *17*, 11.
[131] J. Heikenfeld, A. Jajack, B. Feldman, S. W. Granger, S. Gaitonde, G. Begtrup, B. A. Katchman, *Nat. Biotechnol.* **2019**, *37*, 407.
[132] Y.-H. Lee, D. T. Wong, *Am. J. Dent.* **2009**, *22*, 241.
[133] O. Miočević, C. R. Cole, M. J. Laughlin, R. L. Buck, P. D. Slowey, E. A. Shirtcliff, *Front. Public Health* **2017**, *5*, 133.
[134] G. Matzeu, L. Florea, D. Diamond, *Sens. Actuators, B* **2015**, *211*, 403.
[135] J. Xiao, Y. Liu, L. Su, D. Zhao, L. Zhao, X. Zhang, *Anal. Chem.* **2019**, *91*, 14803.
[136] G. Xiao, J. He, X. Chen, Y. Qiao, F. Wang, Q. Xia, L. Yu, Z. Lu, *Cellulose* **2019**, *26*, 4553.
[137] N. Promphet, J. P. Hinestroza, P. Rattanawaleedirojn, N. Soatthiyanon, K. Siralertmukul, P. Potiyaraj, N. Rodthongkum, *Sens. Actuators, B* **2020**, *321*, 128549.
[138] Z. Zhang, M. Azizi, M. Lee, P. Davidowsky, P. Lawrence, A. Abbaspourrad, *Lab Chip* **2019**, *19*, 3448.
[139] J. Choi, A. J. Bandodkar, J. T. Reeder, T. R. Ray, A. Turnquist, S. B. Kim, N. Nyberg, A. Hourlier-Fargette, J. B. Model, A. J. Aranyosi, S. Xu, R. Ghaffari, J. A. Rogers, *ACS Sens.* **2019**, *4*, 379.
[140] J. He, G. Xiao, X. Chen, Y. Qiao, D. Xu, Z. Lu, *RSC Adv.* **2019**, *9*, 23957.
[141] S. Ardalan, M. Hosseinifard, M. Vosough, H. Golmohammadi, *Biosens. Bioelectron.* **2020**, *168*, 112450.

© 2021 Wiley-VCH GmbH

[142] D. Rodin, M. Kirby, N. Sedogin, Y. Shapiro, A. Pinhasov, A. Kreinin, *Clin. Biochem.* **2019**, *65*, 15.
[143] Y. Cui, W. Duan, Y. Jin, F. Wo, F. Xi, J. Wu, *ACS Sens.* **2020**, *5*, 2096.
[144] Y. Yu, J. Nassar, C. Xu, J. Min, Y. Yang, A. Dai, R. Doshi, A. Huang, Y. Song, R. Gehlhar, A. D. Ames, W. Gao, *Sci. Rob.* **2020**, *5*, eaaz7946.
[145] A. Wiorek, M. Parrilla, M. Cuartero, G. A. Crespo, *Anal. Chem.* **2020**, *92*, 10153.
[146] Y. Lu, K. Jiang, D. Chen, G. Shen, *Nano Energy* **2019**, *58*, 624.
[147] B.-C. Kang, B.-S. Park, T.-J. Ha, *Appl. Surf. Sci.* **2019**, *470*, 13.
[148] H.-Q. Xia, H. Tang, B. Zhou, Y. Li, X. Zhang, Z. Shi, L. Deng, R. Song, L. Li, Z. Zhang, J. Zhou, *Sens. Actuators, B* **2020**, *312*, 127962.
[149] J. Ma, Y. Jiang, L. Shen, H. Ma, T. Sun, F. Lv, A. Kiran, N. Zhu, *Biosens. Bioelectron.* **2019**, *144*, 111637.
[150] C. W. Bae, P. T. Toi, B. Y. Kim, W. I. Lee, H. B. Lee, A. Hanif, E. H. Lee, N.-E. Lee, *ACS Appl. Mater. Interfaces* **2019**, *11*, 14567.
[151] P. T. Toi, T. Q. Trung, T. M. L. Dang, C. W. Bae, N.-E. Lee, *ACS Appl. Mater. Interfaces* **2019**, *11*, 10707.
[152] S.-K. Kim, C. Jeon, G.-H. Lee, J. Koo, S. H. Cho, S. Han, M.-H. Shin, J.-Y. Sim, S. K. Hahn, *ACS Appl. Mater. Interfaces* **2019**, *11*, 37347.
[153] Q. Cao, B. Liang, T. Tu, J. Wei, L. Fang, X. Ye, *RSC Adv.* **2019**, *9*, 5674.
[154] H. Y. Y. Nyein, M. Bariya, L. Kivimäki, S. Uusitalo, T. S. Liaw, E. Jansson, C. H. Ahn, J. A. Hangasky, J. Zhao, Y. Lin, T. Happonen, M. Chao, C. Liedert, Y. Zhao, L.-C. Tai, J. Hiltunen, A. Javey, *Sci. Adv.* **2019**, *5*, eaaw9906.
[155] Y. Lei, W. Zhao, Y. Zhang, Q. Jiang, H. He Jr., A. J. Baeumner, O. S. Wolfbeis, Z. L. Wang, K. N. Salama, H. N. Alshareef, *Small* **2019**, *15*, 1901190.
[156] Q. Xue, Z. Li, Q. Wang, W. Pan, Y. Chang, X. Duan, *Nanoscale Horiz.* **2020**, *5*, 934.
[157] J. Zhao, Y. Lin, J. Wu, H. Y. Y. Nyein, M. Bariya, L.-C. Tai, M. Chao, W. Ji, G. Zhang, Z. Fan, A. Javey, *ACS Sens.* **2019**, *4*, 1925.
[158] X. Zhu, S. Yuan, Y. Ju, J. Yang, C. Zhao, H. Liu, *Anal. Chem.* **2019**, *91*, 10764.
[159] X. He, S. Yang, Q. Pei, Y. Song, C. Liu, T. Xu, X. Zhang, *ACS Sens.* **2020**, *5*, 1548.
[160] W. He, C. Wang, H. Wang, M. Jian, W. Lu, X. Liang, X. Zhang, F. Yang, Y. Zhang, *Sci. Adv.* **2019**, *5*, eaax0649.
[161] A. J. Bandodkar, P. Gutruf, J. Choi, K. Lee, Y. Sekine, J. T. Reeder, W. J. Jeang, A. J. Aranyosi, S. P. Lee, J. B. Model, R. Ghaffari, C.-J. Su, J. P. Leshock, T. Ray, A. Verrillo, K. Thomas, V. Krishnamurthi, S. Han, J. Kim, S. Krishnan, T. Hang, J. A. Rogers, *Sci. Adv.* **2019**, *5*, eaav3294.
[162] A. M. Nightingale, C. L. Leong, R. A. Burnish, S.-U. Hassan, Y. Zhang, G. F. Clough, M. G. Boutelle, D. Voegeli, X. Niu, *Nat. Commun.* **2019**, *10*, 2741.
[163] V. P. Rachim, W.-Y. Chung, *Sens. Actuators, B* **2019**, *286*, 173.
[164] P. Bollella, S. Sharma, A. E. G. Cass, R. Antiochia, *Electroanalysis* **2019**, *31*, 374.
[165] K. O. Kim, G. J. Kim, J. H. Kim, *RSC Adv.* **2019**, *9*, 22790.
[166] J. Hanna, M. Bteich, Y. Tawk, A. H. Ramadan, B. Dia, F. A. Asadallah, A. Eid, R. Kanj, J. Costantine, A. A. Eid, *Sci. Adv.* **2020**, *6*, eaba5320.
[167] M. Porumb, S. Stranges, A. Pescapè, L. Pecchia, *Sci. Rep.* **2020**, *10*, 170.
[168] A. K. Singh, S. K. Jha, *IEEE Sens. J.* **2019**, *19*, 8332.
[169] L. F. De Castro, S. V. De Freitas, L. C. Duarte, J. A. C. De Souza, T. R. L. C. Paixão, W. K. T. Coltro, *Anal. Bioanal. Chem.* **2019**, *411*, 4919.
[170] L. García-Carmona, A. Martín, J. R. Sempionatto, J. R. Moreto, M. C. González, J. Wang, A. Escarpa, *Anal. Chem.* **2019**, *91*, 13883.
[171] J. Chen, X. Zhu, Y. Ju, B. Ma, C. Zhao, H. Liu, *Sens. Actuators, B* **2019**, *285*, 56.
[172] B. Gao, Z. He, B. He, Z. Gu, *Sens. Actuators, B* **2019**, *288*, 734.
[173] J. R. Sempionatto, L. C. Brazaca, L. García-Carmona, G. Bolat, A. S. Campbell, A. Martin, G. Tang, R. Shah, R. K. Mishra, J. Kim, V. Zucolotto, A. Escarpa, J. Wang, *Biosens. Bioelectron.* **2019**, *137*, 161.
[174] J. Choi, R. Ghaffari, L. B. Baker, J. A. Rogers, *Sci. Adv.* **2018**, *4*, eaar3921.
[175] Z. Sonner, E. Wilder, J. Heikenfeld, G. Kasting, F. Beyette, D. Swaile, F. Sherman, J. Joyce, J. Hagen, N. Kelley-Loughnane, R. Naik, *Biomicrofluidics* **2015**, *9*, 031301.
[176] J. Zhang, M. Rupakula, F. Bellando, E. Garcia Cordero, J. Longo, F. Wildhaber, G. Herment, H. Guérin, A. M. Ionescu, *ACS Sens.* **2019**, *4*, 2039.
[177] A. Jajack, M. Brothers, G. Kasting, J. Heikenfeld, *PLoS One* **2018**, *13*, e0200009.
[178] Y. J. Hong, H. Lee, J. Kim, M. Lee, H. J. Choi, T. Hyeon, D.-H. Kim, *Adv. Funct. Mater.* **2018**, *28*, 1805754.
[179] H. Lee, C. Song, Y. S. Hong, M. S. Kim, H. R. Cho, T. Kang, K. Shin, S. H. Choi, T. Hyeon, D.-H. Kim, *Sci. Adv.* **2017**, *3*, e1601314.
[180] S. Emaminejad, W. Gao, E. Wu, Z. A. Davies, H. Yin Yin Nyein, S. Challa, S. P. Ryan, H. M. Fahad, K. Chen, Z. Shahpar, S. Talebi, C. Milla, A. Javey, R. W. Davis, *Proc. Natl. Acad. Sci. U. S. A.* **2017**, *114*, 4625.
[181] A. J. Bandodkar, W. Jia, C. Yardımcı, X. Wang, J. Ramirez, J. Wang, *Anal. Chem.* **2015**, *87*, 394.
[182] E. Cho, M. Mohammadifar, S. Choi, in *2017 IEEE 30th Int. Conf. Micro Electro Mechanical Systems (MEMS)*, IEEE, Piscataway, NJ **2017**, pp. 366–369.
[183] G. Liu, C. Ho, N. Slappey, Z. Zhou, S. E. Snelgrove, M. Brown, A. Grabinski, X. Guo, Y. Chen, K. Miller, J. Edwards, T. Kaya, *Sens. Actuators, B* **2016**, *227*, 35.
[184] S. Yin, Z. Jin, T. Miyake, *Biosens. Bioelectron.* **2019**, *141*, 111471.
[185] J. Xiao, Y. Liu, L. Su, *Anal. Chem.* **2019**, *91*, 14803.
[186] X. Zhu, Y. Ju, J. Chen, D. Liu, H. Liu, *ACS Sens.* **2018**, *3*, 1135.
[187] O. Parlak, S. T. Keene, A. Marais, V. F. Curto, A. Salleo, *Sci. Adv.* **2018**, *4*, eaar2904.
[188] H. Y. Y. Nyein, W. Gao, Z. Shahpar, S. Emaminejad, S. Challa, K. Chen, H. M. Fahad, L.-C. Tai, H. Ota, R. W. Davis, A. Javey, *ACS Nano* **2016**, *10*, 7216.
[189] X.-Y. Xu, B. Yan, X. Lian, *Nanoscale* **2018**, *10*, 13722.
[190] Y. Guan, S. Qu, B. Li, L. Zhang, H. Ma, L. Zhang, *Biosens. Bioelectron.* **2016**, *77*, 124.
[191] R. M. Taylor, P. R. Miller, P. Ebrahimi, R. Polsky, J. T. Baca, *Lab. Anim.* **2018**, *52*, 526.
[192] P. P. Samant, M. R. Prausnitz, *Proc. Natl. Acad. Sci. U. S. A.* **2018**, *115*, 4583.
[193] J. P. Bantle, W. Thomas, *J. Lab. Clin. Med.* **1997**, *130*, 436.
[194] P. J. Stout, N. Peled, B. J. Erickson, M. E. Hilgers, J. R. Racchini, T. B. Hoegh, *Diabetes Technol. Ther.* **2001**, *3*, 81.
[195] P. P. Samant, M. M. Niedzwiecki, N. Raviele, V. Tran, J. Mena-Lapaix, D. I. Walker, E. I. Felner, D. P. Jones, G. W. Miller, M. R. Prausnitz, *Sci. Transl. Med.* **2020**, *12*, eaaw0285.
[196] A. M. Nightingale, C. L. Leong, R. A. Burnish, S.-U. Hassan, Y. Zhang, G. F. Clough, M. G. Boutelle, D. Voegeli, X. Niu, *Nat. Commun.* **2019**, *10*, 2741.
[197] C.-Z. Zhang, X.-Q. Cheng, J.-Y. Li, P. Zhang, P. Yi, X. Xu, X.-D. Zhou, *Int. J. Oral Sci.* **2016**, *8*, 133.
[198] S. Chiappin, G. Antonelli, R. Gatti, E. F. De Palo, *Clin. Chim. Acta* **2007**, *383*, 30.
[199] S. Saha, H. Cano-Garcia, I. Sotiriou, O. Lipscombe, I. Gouzouasis, M. Koutsoupidou, G. Palikaras, R. Mackenzie, T. Reeve, P. Kosmas, E. Kallos, *Sci. Rep.* **2017**, *7*, 6855.
[200] H. Choi, S. Luzio, A. Porch, in *2017 IEEE MTT-S International Microwave Symposium (IMS)*, IEEE, Piscataway, NJ **2017**, pp. 876–879.
[201] J. Grammes, E. Küstner, A. Dapp, M. Hummel, J.-C. Kämmer, T. Kubiak, I. Schütz-Fuhrmann, S. Zimny, E. Bollow, R. W. Holl, *Diabetic Med.* **2020**, *37*, 856.

© 2021 Wiley-VCH GmbH

Le Minh Tu Phan is currently an assistant professor of Biochemistry at Gachon University, Republic of Korea, as well as University Lecturer at the University of Danang, Vietnam. He received his Master of Medicine in Functional Medicine at Hue University of Medicine and Pharmacy, Vietnam in 2014, and obtained his Ph.D. degree in Biochemistry at Chung-Ang University, Korea in 2020. He is presently working in clinical biochemistry and interested in developing superior biosensing platforms applicable to medical diagnostic application, especially point-of-care diagnostic devices, based on advanced nanobiomaterials.

Sungbo Cho is a professor of the Electronic Engineering at Gachon University, Seongnam, Korea. He received his B.S. and M.S. in Electrical Engineering at Korea University in 2001, Republic of Korea and Dr.-Ing. degree in Physics and Mechatronics at Saarland University/Fraunhofer Institute for Biomedical Engineering, Germany in 2008. His interest has been focused on the biomicro-electromechanical systems manipulating DNA, protein, cells, or tissues & bioimpedance characterizing nondestructive and real-time electrical properties. His research topics are from basic understanding of biology to fabrication of in vitro/vivo sensors and electronic devices for clinical applications.

© 2021 Wiley-VCH GmbH